

Nuclear envelope tethering inhibits the formation of ALT-associated PML bodies in ALT cells

Chia-Wei Yang¹, Meng-Hsun Hsieh¹, Hao-Jhe Sun¹, Shu-Chun Teng^{1,2}

¹Department of Microbiology, College of Medicine, National Taiwan University, Taipei 10051, Taiwan

²Center of Precision Medicine, National Taiwan University, Taipei 10051, Taiwan

Correspondence to: Shu-Chun Teng; **email:** shuchunteng@ntu.edu.tw

Keywords: alternative lengthening of telomeres, telomere-telomere recombination, nuclear envelope tethering, SUN1, RAP1

Received: August 29, 2020

Accepted: February 16, 2021

Published: April 4, 2021

Copyright: © 2021 Yang et al. This is an open access article distributed under the terms of the [Creative Commons Attribution License](https://creativecommons.org/licenses/by/3.0/) (CC BY 3.0), which permits unrestricted use, distribution, and reproduction in any medium, provided the original author and source are credited.

ABSTRACT

Telomere length homeostasis is essential for maintaining genomic stability and cancer proliferation. Telomerase-negative cancer cells undergo recombination-mediated alternative lengthening of telomeres. Telomeres associate with the nuclear envelope through the shelterin RAP1 and nuclear envelope SUN1 proteins. However, how the associations between telomeres and the nuclear envelope affect the progression of telomere recombination is not understood. Here, we show that telomere anchorage might inhibit telomere-telomere recombination. SUN1 depletion stimulates the formation of alternative lengthening of telomeres-associated promyelocytic leukemia bodies in ALT cells. In contrast, overexpression of a telomere-nuclear envelope-tethering chimera protein, RAP1-SUN1, suppresses APB formation. Moreover, inhibition of this nuclear envelope attachment alleviates the requirement of TOP3 α for resolving the supercoiling pressure during telomere recombination. A coimmunoprecipitation assay revealed that the SUN1 N-terminal nucleoplasmic domain interacts with the RAP1 middle coil domain, and phosphorylation-mimetic mutations in RAP1 inhibit this interaction. However, abolishing the RAP1-SUN1 interaction does not hinder APB formation, which hints at the existence of another SUN1-dependent telomere anchorage pathway. In summary, our results reveal an inhibitory role of telomere-nuclear envelope association in telomere-telomere recombination and imply the presence of redundant pathways for the telomere-nuclear envelope association in ALT cells.

INTRODUCTION

Telomeres protect the ends of linear chromosomes from end-to-end fusion, injurious chromosomal rearrangements, and genomic instability [1]. Human telomeric DNA is composed of a serial of hexameric DNA repeats (5'-TTAGGG-3') that are synthesized by telomerase, an RNA-protein complex [2, 3]. In normal conditions, the telomeres of most human somatic cells are continuously shortened during each cell division due to the absence of telomerase and incomplete replication. When telomeres become extremely short, they lose protection abilities and are recognized as broken-ends, which turn on cell cycle checkpoint signaling. In human fibroblasts, gradually losing telomeres induce chromosome fusion, crisis, and apoptosis [4]. Cancer

cells can circumvent this crisis through the reactivation of telomerase (85%) or the alternative lengthening of telomeres [5] recombination pathway (15%) to elongate their telomeres [6–8]. Many DNA repair and recombination proteins have been discovered in the ALT pathway, but the molecular mechanisms and regulations of ALT are still not fully understood [6, 9].

ALT cells possess a unique marker, ALT-associated promyelocytic leukemia (PML) bodies (APBs), containing telomeric DNA as well as many DNA repair and replication proteins, such as RAD52, RAD51, RAD50, RPA, TRF1, TRF2, and NBS1 [10]. Many studies speculated that APBs provide a “recombinogenic microenvironment” to benefit ALT formation [11–19]. APBs can be detected within a

mitotic cell cycle [20], and seem to be dynamic in the nucleus [19–22]. High-resolution images revealed that APB-associated telomere clustering promotes telomere-telomere recombination after replication [23]. A recent study showed that telomeric DNA synthesis exclusively occurs in APBs [18]. In addition to APBs, another characteristic of ALT cells is the presence of the high content of extrachromosomal telomeric DNA circles, especially single-stranded C-rich circles (C-circles) [14, 24–30]. Nonetheless, how the C-circles are generated remains mysterious.

The telomere-associated shelterin proteins TRF1, TRF2, TIN2, and RAP1 act as negative regulators of telomere length in telomerase-positive cells to assure the telomeric integrity [31]. They are also important for APB formation [10, 32, 33]. Knockout mice studies showed that loss of RAP1 increases the frequency of telomeric sister chromatid exchanges (T-SCEs) in mouse embryonic fibroblasts (MEFs), suggesting that RAP1 is critical for the repression of telomeric recombination in MEFs [34, 35]. However, the mechanism of how shelterin RAP1 regulates telomere-telomere recombination in ALT cancer cells remains to be clarified.

Linkers of nucleoskeleton and cytoskeleton (LINC) complexes are conserved nuclear membrane proteins that span in the nuclear envelope to connect cytoskeletal and nucleoskeletal elements [36, 37]. The LINC complexes play critical roles in multiple fundamental cellular processes, including nuclear migration, meiotic chromosome pairing, mechanotransduction, and nuclear shape maintenance [38]. The LINC complexes consist of the conserved inner nuclear membrane SUN proteins and outer nuclear membrane KASH proteins [36]. They are involved in the chromatin mobility, mobility, and clusters of DNA breaks, and double-strand break repair [39–43]. SUN1 and SUN2 were the first identified SUN proteins that are widely expressed in mammals [44–47]. The N-terminal domain of SUN1 locates in the nucleoplasm, while its C-terminal domain is inserted into the perinuclear space for docking the KASH proteins [36, 37]. Immunohistological data showed that SUN1 expression was reduced in breast cancer tissues and cell lines as compared to the normal mammary gland tissues, suggesting that reduction of SUN1 plays a pathological role in breast cancer formation [48]. SUN1 is also important for messenger RNA export, nuclear pore complex distribution, and nucleolar morphogenesis [49–52].

Telomeres of T-lymphocytes are positioned within the interior 50% of the nuclear volume [53]. Other studies showed that telomeres seem to attach to the nuclear matrix during interphase in non-ALT cells [54–56].

Surprisingly, it was later revealed that telomeres can attach to the nuclear envelope during the mitotic cell cycle through the interaction between RAP1 and SUN1 in HeLa and IMR90 cells [57]. On the contrary, telomere tethering to the nuclear envelope in ALT cells has not been examined. We were curious about whether telomere tethering affects the telomere-telomere recombination pathway in ALT cells.

In this study, we found that depletion of the nuclear envelope SUN1 promotes the APB formation and C-circle levels in ALT cells. On the other hand, the APB formation is impaired when the telomeres are forced to link with the nuclear envelope, suggesting that the telomere-nuclear envelope attachment may prevent telomere-telomere recombination. SUN1 knockdown recovers the deficiency of the APB formation in the TOP3 α -depleted cells, suggesting that the reduction of the nuclear membrane tethering may partially relieve the requirement of TOP3 α during telomere-telomere recombination. Moreover, our data imply a SUN1-dependent but RAP1-independent telomere-tethering pathway that may also prevent telomere-telomere recombination in ALT cells.

MATERIALS AND METHODS

Cell culture, transfections, and methionine treatments

HEK-293T, U2OS, VA13, HeLa, and HCT116 cells were cultured in Dulbecco's modified Eagle's medium (DMEM) supplemented with 10% fetal bovine serum, penicillin, streptomycin, and nonessential amino acids (HyClone). Transfection was conducted using T-Pro nonliposome transfection reagent II (T-Pro Biotechnology). To increase the APB formation ratio, virus-infected U2OS and VA13 cells were treated with methionine restriction as previously described [33]. In brief, cells were grown on glass coverslips in DMEM to 50% confluency. The cells were washed once with methionine-deficient medium before incubation in methionine-deficient medium for 3 days; this methionine-deficient DMEM (Gibco) contained 10% fetal bovine serum, penicillin, streptomycin, 4 mM glutamine, nonessential amino acids (HyClone), and L-cysteine (48 mg/l, Sigma).

Viral infection

HEK-293T cells were cotransfected with the packaging plasmid (pCMV- Δ 8.91), envelope (pMD.G), and either hairpin pLKO-RNAi vectors or cDNA expression pLAS5w.Pneo vectors (National RNAi Core Facility, Institute of Molecular Biology/Genomic Research Centre, Academia Sinica, Taiwan) for virus production.

The specific oligo sequences of the shRNA are listed in Supplementary Table 1. Twenty-four hours posttransfection, the medium was replaced with DMEM containing 1% BSA. Virus-containing supernatants were collected at 48 h and 72 h posttransfection. The cells were infected with viruses and cultured in DMEM containing 1 µg/ml polybrene (Millipore) for 16 h. The transduced cells were selected with DMEM containing 1 µg/ml puromycin (Invitrogen) or G418 (Sigma) for the indicated days (600 µg/ml G418 for VA13 cells and 800 µg/ml G418 for U2OS cells).

Plasmid construction

The primers used in this study are listed in Supplementary Table 2. For pcDNA3HA-RAP1 construction, *RAP1* cDNA was amplified from U2OS cell cDNA by PCR using the primers RAP1-BamHI-1F and RAP1-XhoI-R and then cloned into the BamHI-XhoI sites of pcDNA3HA (a gift from Dr. Tsai-Kun Li). For pLAS5w-RAP1 construction, *RAP1* cDNA was amplified by PCR using the primers RAP1-NheI-For and RAP1-NsiI-Rev and then cloned into the NheI-NsiI sites of pLAS5w.Pneo (National RNAi Core Facility, Institute of Molecular Biology/Genomic Research Centre, Academia Sinica, Taiwan). The pcDNA3HA-RAP1 and pLAS5w-RAP1 truncated mutants were generated using a QuickChange site-directed mutagenesis kit (Stratagene) with the primers listed in Supplementary Table 2. The pEGFP-SUN1 N205 plasmid was generated by self-ligation of SmaI-digested pEGFP-SUN1 (a gift from Dr. Angelika A. Noegel), which removes the SUN1 C-terminus. For pLAS5w-SUN1 construction, *SUN1* cDNA was amplified from pEGFP-SUN1 by PCR using the primers NheI-SUN1-For and SUN1-EcoRI-Rev and then cloned into the NheI-EcoRI sites of a pLAS5w.Pneo plasmid. The pLAS5w-RAP1-SUN1 fusion was constructed as follows: the *RAP1*-G8 sequence was amplified by PCR using the primers HpaI-RAP1-For and RAP1-G8-NheI-Rev, which contain the sequence for eight glycine residues before the NheI site at the 3' end of the reverse primer, and then cloned into HpaI-NheI in pLAS5w.Pneo to create pLAS5w-RAP1-G8. Next, *SUN1* cDNA was amplified by PCR using the primers NheI-SUN1-For and SUN1-EcoRI-Rev and inserted into the NheI-EcoRI sites of pLAS5w-RAP1-G8 to obtain pLAS5w-RAP1-SUN1. To create RAP1 ΔC, which cannot interact with TRF2 [58], RAP1 amino acid 1-289 sequences were amplified by PCR using the primers HpaI-RAP1-For and RCTdel-G8-NheI-Rev. The 3' end of the reverse RCTdel-G8-NheI-Rev primer contains the sequence for eight glycine residues before the NheI site. The PCR-amplified HpaI- and NheI-digested RAP1 ΔC fragments were cloned into pLAS5w-SUN1 to obtain pLAS5w-RAP1ΔC-SUN1.

The RAP1 8FA and RAP1 8DE sequences were synthesized by gBlocks® gene fragments (Integrated DNA Technologies) and then cloned into the pcDNA3HA and pLAS5w plasmids, respectively. All plasmids were sequenced before use.

Cell fixation and immunofluorescence assays

Cells were seeded on glass coverslips coated with 0.2% gelatin (Sigma). After washing with phosphate-buffered saline (PBS), the cells were fixed in 4% paraformaldehyde in PBS for 10 min at room temperature. The fixed cells were permeated with 0.05% Triton X-100 in PBS for 5 min. These cells were washed three times with PBS and incubated with 1% BSA in PBS for 1 h at room temperature. For immunostaining, cells were incubated for 2 h with anti-TRF2 (1:200, clone 4A794, Millipore) and anti-PML (1:150, N-19, sc9862, Santa Cruz Biotechnology) primary antibodies at room temperature. The cells were washed twice with PBS for 5 min each time and then incubated with chicken anti-goat Alexa Fluor 594 (Invitrogen) for 1 h at room temperature. The cells were washed twice with PBS and incubated with goat anti-mouse Alexa Fluor 488 (Invitrogen) and 4',6-diamidino-2-phenylindole (DAPI) (Sigma) for 1 h at room temperature. The cells were washed three times with PBS and mounted on glass slides. Immunofluorescence images were acquired with a Zeiss Axioplan fluorescence microscope.

Immunoblotting

Cell lysates were prepared in sample buffer, separated by sodium dodecyl sulfate-polyacrylamide gel electrophoresis (SDS-PAGE), and transferred to a PVDF membrane. The primary antibodies used in this study were anti-GAPDH (GTX100118, GeneTex), anti-Lamin A/C (N-18, sc-6215), anti-SUN1 (EPR6554, ab124770, Abcam), anti-RAP1 (A300-306A, Bethyl Laboratories), and anti-TOP3α (14525-1-AP, Proteintech). Horseradish peroxidase (HRP)-conjugated sheep anti-mouse and donkey anti-rabbit antibodies (GE Healthcare) were used as secondary antibodies. Immunoreactivity was detected by chemiluminescence using X-ray film (Fujifilm Corporation).

C-circle assay

The C-circle assay was performed as previously described [26]. Briefly, each DNA sample (10 and 40 ng) was incubated with or without 7.5 U φ29 DNA polymerase (NEB, M0269) in a 20-µl reaction mixture containing 9.25 µl of 2.16x master mix (8.65 mM DTT, 2.16x φ29 buffer, 8.65 µg/ml BSA, 0.216% v/v Tween 20, 2.16 mM dATP, 2.16 mM dGTP, 2.16 mM dTTP,

and 2.16 mM dCTP) for performing the rolling circle amplification reaction at 30° C for 8 h and then transferred to 70° C for 20 min to inactivate φ29 DNA polymerases. The reaction mixture without the addition of φ29 DNA polymerase was used as a control. The reaction mixtures were loaded onto an Amersham Hybond-N+ membrane using the Bio-Rad Bio-Dot system. The membrane was cross-linked with 454 nm UV-C at 1,200 J twice and hybridized overnight with a ³²P-labeled (Invitrogen) CCA oligonucleotide probe (5'-CTAACCCTAACCCCTAACCC-3') in hybridization buffer (225 mM NaCl; 15 mM NaH₂PO₄; 1.5 mM EDTA, pH 7.6; 10% polyethylene glycol 8000; and 7% SDS) at 37° C. The membrane was washed three times with washing solution (0.5 × SSC, 0.1% SDS) and exposed to X-ray film (Fujifilm Corporation). The images were quantified using NIH ImageJ software.

Immunoprecipitation

Cells were lysed in lysis buffer (150 mM NaCl; 1% Triton X-100; 50 mM Tris-HCl, pH 8.0; 1 mM PMSF; Roche protease inhibitor; and a phosphatase inhibitor cocktail) on ice for 10 min. After centrifugation at 13,000 rpm for 10 min at 4° C, 1 mg of protein lysate was incubated with 50 μl of μMACS anti-GFP microbeads (Miltenyi Biotec) for 1 hour at 4° C. Labeled proteins were applied to a μMACS column placed in a μMACS separator (Miltenyi Biotec). Then, the column was washed three times with Wash Buffer 1 (150 mM NaCl, 1% NP-40, 0.5% sodium deoxycholate, 0.1% SDS, and 50 mM Tris-HCl, pH 8.0) and further washed once with 20 mM Tris-HCl, pH 7.5. The target proteins were eluted in 50 μl elution buffer preheated to 95° C (50 mM Tris-HCl, pH 6.8; 50 mM DTT; 1% SDS, 1 mM EDTA; 0.005% bromophenol blue; and 10% glycerol) for SDS-PAGE analysis.

Telomere restriction fragment (TRF) analysis

Genomic DNA was extracted from cells by a genomic DNA purification kit (Promega). Genomic DNA (2 μg) was digested with RsaI and HinfII (New England Biolabs), and run on a 0.5% UltraPure™ Agarose gel (Invitrogen) in 0.5 × TBE buffer using a Thermo Scientific™ Owl™ A1 Large Gel System (Invitrogen) at 120 V for 20 h. The gel was soaked in 0.25 N HCl for 15 min to denature the DNA and then neutralized in a 0.5 N NaOH and 1.5 M NaCl solution for 30 min. The digested DNA was transferred onto a Hybond N+ nylon membrane (GE healthcare). The membrane was cross-linked twice with 454 nm UV-C at 1,200 J twice and hybridized overnight with a ³²P-labeled (Invitrogen) 800-bp TTACCC telomere-specific probe in Church buffer (1% BSA, 1 mM EDTA, 0.5 M phosphate buffer, and 7% SDS) at 65° C. The next day, the blot was

washed three times with 4 × SSC buffer and then exposed to X-ray film (Fujifilm Corporation). Telomere length was determined by ImageQuant TL software (GE healthcare).

Statistical analysis

Each experiment was repeated at least three times. The results are expressed as the means ± standard deviation (SD). A two-tailed Student's t-test was used for statistical analysis. *P* < 0.05 was considered statistically significant.

RESULTS

Depletion of SUN1 promotes APB and C-circle formation in ALT cells

The role of SUN1 in telomere-nuclear envelope anchorage in non-ALT cells [57] prompted us to investigate whether SUN1 is required for telomere-telomere recombination in ALT cells. We first examined the significance of SUN1 in the viability of U2OS and VA13 ALT cells. Depletion of SUN1 slowed the growth of both ALT cell lines (Supplementary Figure 1A, 1B). Similar to SUN1-depleted ALT cells, cell growth was also reduced in SUN1-depleted telomerase-positive cells (Supplementary Figure 1C, 1D). The growth defect caused by SUN1 depletion was previously reported in SUN1-suppressed HeLa1.2.11 cells. SUN1 knockdown can induce robust activation of the checkpoint response and has a dramatic effect on the cell cycle [57]. The dramatic growth defect induced by SUN1 depletion hindered us from observing long-term telomere length alterations in SUN1-depleted cells. However, the short-term depletion of SUN1 did not destroy the integrity of the nuclear lamina (Supplementary Figure 2). These results suggest that SUN1 plays a role in cell growth and the cell cycle.

One of the signatures of ALT cells is the formation of APBs, but the mechanism of their formation remains unclear [10, 22]. To understand the function of SUN1 in the ALT pathway, we studied the formation of APBs by examining the colocalization of PML and the telomere-binding protein TRF2. The SUN1 protein levels in the short-term SUN1-depleted U2OS and VA13 ALT cells were confirmed by immunoblotting (Figure 1A). The percentage of the APB-positive cells in the SUN1-depleted ALT cells was significantly increased (Figure 1B, 1C). Under SUN1 depletion, the percentage of the cells exhibiting another ALT cell biomarker, the C-circle [25], was also significantly increased (Figure 1D, 1E). In contrast, no APB formation was observed in the SUN1-depleted telomerase-positive HeLa and HCT116 cells, implying that the loss of SUN1 does not convert

telomere-positive cells into telomerase-negative ALT cells (Supplementary Figure 3). These results suggest that SUN1 may play an inhibitory role in the formation of APBs and C-circles.

The RAP1-SUN1 fusion protein decreases APB formation

Since the interaction between the nuclear envelope SUN1 protein and telomere shelterin RAP1 protein contributes to the tethering of human telomeres to the nuclear envelope in non-ALT cells [57], we speculated that enhancing telomere-nuclear envelope interactions

may decrease APB formation in ALT cells. To test this hypothesis, we generated a RAP1-SUN1 fusion protein (Figure 2A) that connects RAP1 and SUN1 via an eight-glycine linker. The RAP1-SUN1 fusion protein was overexpressed in U2OS and VA13 ALT cells through lentivirus transduction, and the expression levels of the fusion and endogenous proteins were measured with immunoblotting (Figure 2B). It was reported that APBs are usually found in less than 5% of an asynchronous ALT cell population [33]. However, methionine deprivation can arrest cells in the G2 phase and increase the number of APBs in ALT cells [15, 59]. To monitor with efficiency the difference in APB

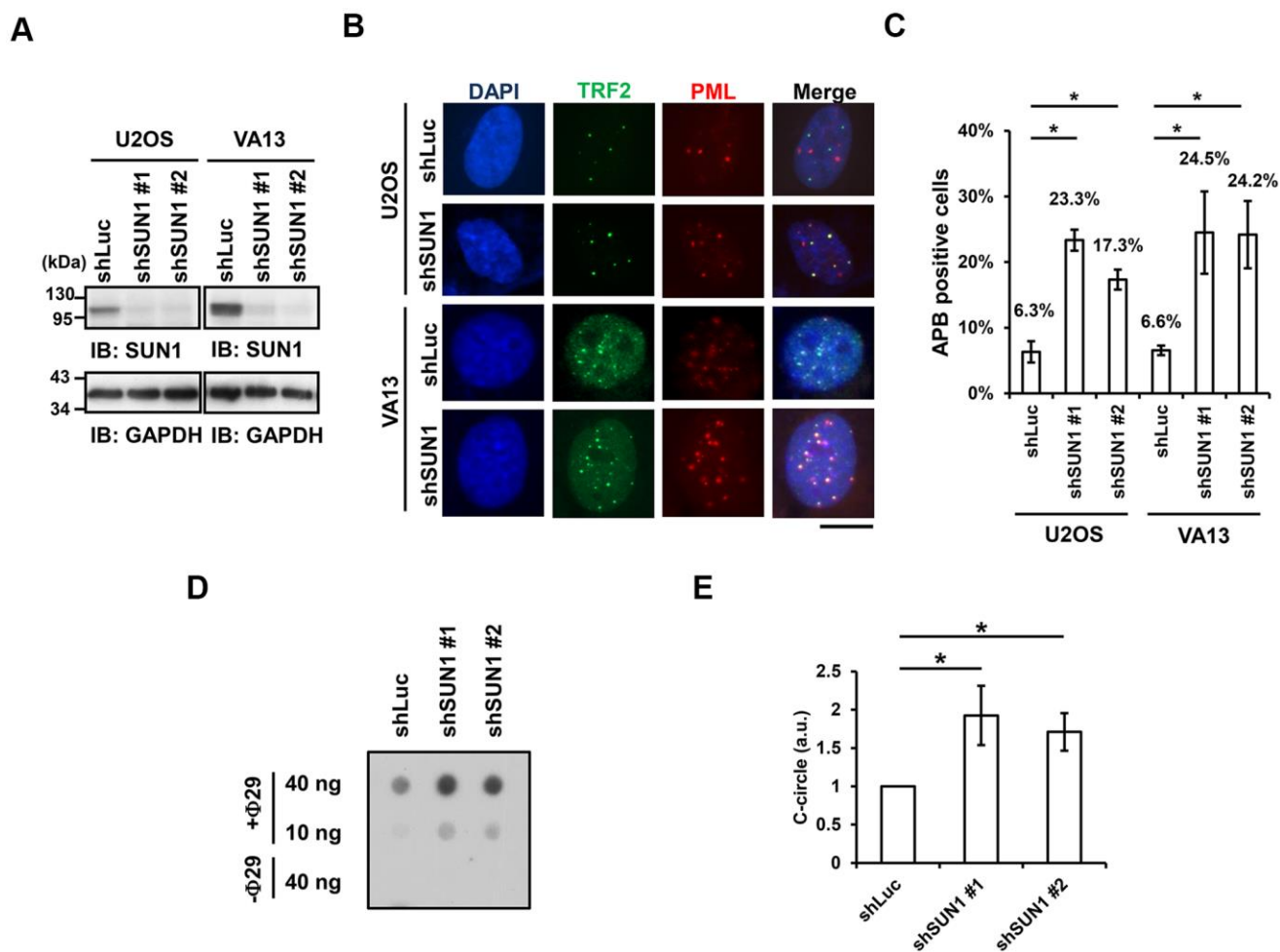


Figure 1. SUN1 knockdown induces APB formation and C-circle levels. (A) U2OS and VA13 cells were infected with control (shLuc) or shSUN1 lentivirus and selected with 1 μ g/ml puromycin for 3 days. Cell lysates were subjected to immunoblot analysis with anti-SUN1 and anti-GAPDH antibodies. GAPDH was used as the loading control. (B) Representative images show the colocalization of TRF2 and PML in U2OS cells (upper panel) and VA13 cells (bottom panel). Virus-infected and puromycin-selected cells were subjected to immunofluorescence staining with anti-TRF2 and anti-PML antibodies. DNA was stained with DAPI. Cells containing at least three large TRF2 and PML colocalization foci (yellow) in the nucleus were counted as APB-positive cells. Scale bar, 20 μ m. (C) Quantification of APBs (%) in the U2OS and VA13 cells shown in (B). Approximately 200-300 cells were analyzed for each independent experiment. Error bars denote SD; n=3 (independent experiments); * P <0.05 (two-tailed Student's t-test). (D) Depletion of SUN1 stimulates the formation of C-circles in U2OS cells. (E) Quantification of the level of C-circles in the cells in (D). The signals were quantified with ImageJ software. The level of C-circles is represented in an arbitrary unit (a.u.). Error bars denote SD; n=3 (independent experiments); * P <0.05 (two-tailed Student's t-test).

formation between the cells expressing the empty vector and RAP1-SUN1, we depleted methionine in the virus-transduced U2OS and VA13 ALT cells. Overexpression of SUN1 or RAP1 alone did not affect the APB formation (Figure 2C, 2D and Supplementary Figure 4). Coimmunostaining of RAP1 and Lamin A/C demonstrated that the RAP1-SUN1 fusion protein was localized to the nuclear periphery (Supplementary Figure 5A). The DNA-binding protein TRF2 binds to telomeric DNA directly and interacts with RAP1 to form the shelterin complex [58]. Interestingly, some TRF2 proteins localize around the periphery of the

nucleus, implying that the function of the RAP1 in the RAP1-SUN1 fusion protein is competent to attract TRF2 to the nuclear envelope (Supplementary Figure 5B). Overexpression of the RAP1-SUN1 fusion protein significantly reduces the APBs formation in both ALT cells (Figure 2C, 2D). Notably, the APB foci were primarily formed in the internal region of the nucleus but rarely in the periphery. Additionally, overexpression of the RAP1-SUN1 fusion protein slowed the cell growth of the ALT- and telomerase-positive cells (Supplementary Figure 6). RAP1 interacts with TRF2 through its RAP1 C-terminal (RCT) protein-protein

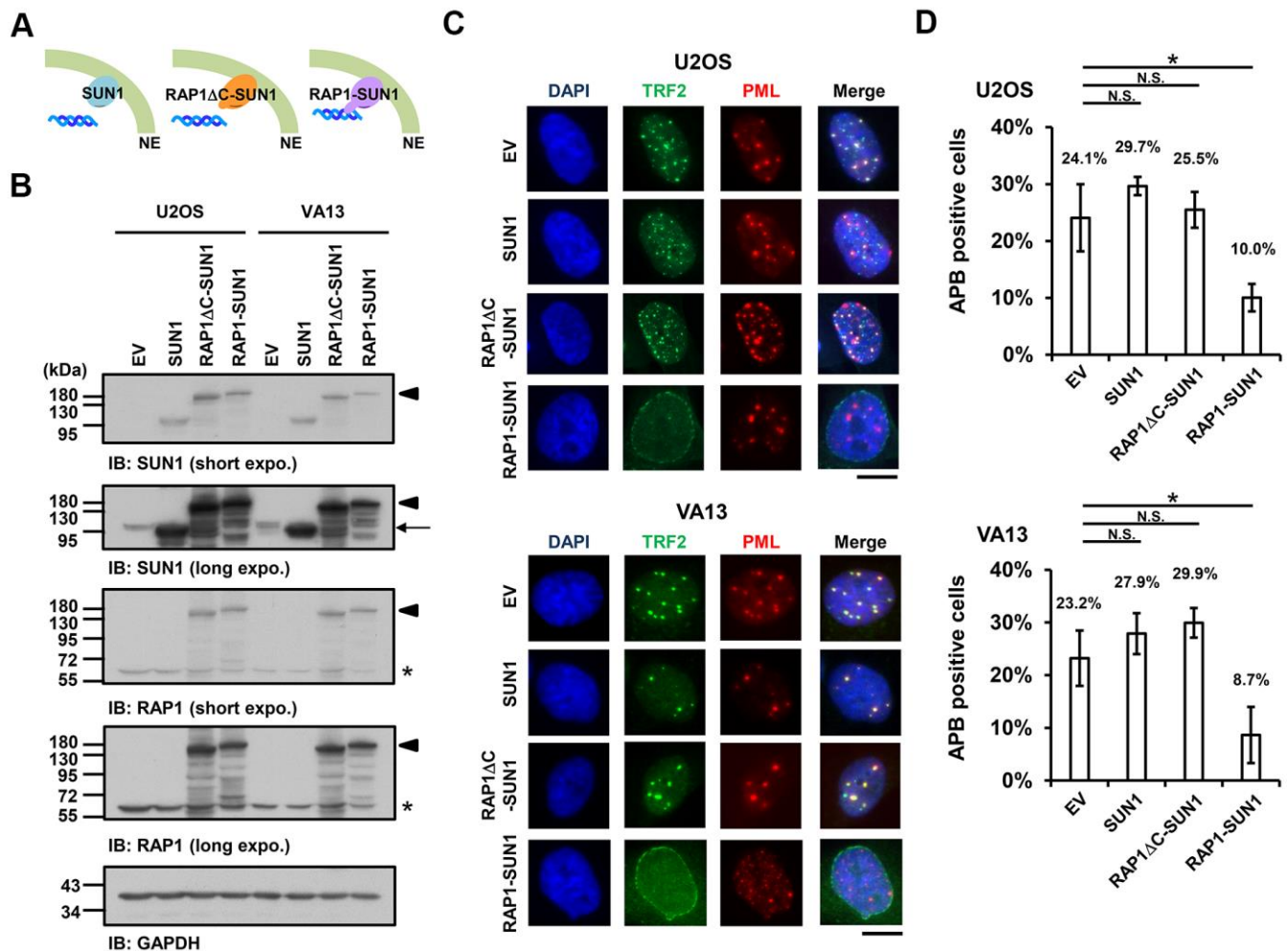


Figure 2. The enhancement of nuclear envelope anchorage inhibits APB formation. (A) Schematic diagrams of cells overexpressing SUN1, RAP1-RCT-domain-deleted-SUN1 (RAP1ΔC-SUN1), or RAP1-SUN1 fusion chimera protein are shown. NE, the nuclear envelope. (B) U2OS and VA13 cells were infected with lentivirus expressing the empty vector control (EV), SUN1, RAP1ΔC-SUN1, or RAP1-SUN1 fusion and then selected in medium containing G418 for 5 days. Cell lysates were analyzed by immunoblotting with anti-RAP1, anti-SUN1, and anti-GAPDH antibodies. The arrowhead indicates the RAP1-SUN1 fusion protein. The arrow indicates endogenous SUN1. The asterisk indicates endogenous RAP1. The ladders under the major protein band show possible products of protein degradation. GAPDH was used as the loading control. (C) Representative images show the colocalization of TRF2 and PML in U2OS cells (upper panel) and VA13 cells (bottom panel), as shown in Figure 1. Scale bar, 20 μm. (D) Quantification of APBs (%) in the U2OS and VA13 cells shown in (C). Approximately 200-300 cells were analyzed for each independent experiment. Error bars denote SD; n=3 (independent experiments); *P<0.05 (two-tailed Student's t-test). N.S., no significance.

interaction domain [58]. To examine whether the interaction between RAP1 and TRF2 affects telomere anchorage, we generated the RCT domain-deleted RAP1-SUN1 fusion protein (RAP1 Δ C-SUN1) (Figure 2B), which loses the ability of RAP1 to bind to telomeres. As predicted, similar to SUN1 overexpression, RAP1 Δ C-SUN1 fusion protein expression did not affect APB formation (Figure 2C, 2D). However, the C-circle levels were not changed in the cells overexpressing RAP1, SUN1, RAP1 Δ C-SUN1, or RAP1-SUN1 fusion protein (Supplementary Figure 7). These results indicate that the imposed telomere-nuclear envelope interaction might impede the progression of APB formation.

SUN1 depletion and RAP1-SUN1 fusion do not affect telomere length during short-term culturing

Because of the growth defect in SUN1-knockdown or RAP1-SUN1-overexpressing cells, we could not acquire long-term cultured ALT cells. We could merely obtain short-term cultured U2OS ALT cells. To evaluate whether telomere length was affected by SUN1 depletion or RAP1-SUN1 overexpression in these short-term-cultured ALT cells, we performed a telomere restriction fragment (TRF) assay. The telomere length in SUN1-depleted cells was not changed after seven days (Supplementary Figure 8A). We next measured the telomere length of SUN1-, RAP1 Δ C-SUN1-, and RAP1-SUN1-overexpressing cells. The telomere lengths in these cells did not show significant variation compared to those in the control cells (Supplementary Figure 8B). These results reveal that telomere length homeostasis is not changed in SUN1-depleted or RAP1-SUN1-overexpressed short-term cultures.

Depletion of SUN1 alleviates the requirement of TOP3 α in ALT cell

Previous studies demonstrated that telomere-telomere recombination specifically requires TOP3 α to resolve highly negative topological stress generated during fork movement along telomeres undergoing recombination [60, 61]. If the supercoiling stress is at least partly derived from the anchorage of telomeres to the nuclear envelope, detaching the telomeres from the nuclear envelope may allow free rotation of the telomeres during recombination and thereby relieve the supercoiling tension. To examine this possibility, we depleted TOP3 α in ALT cells to evaluate the APB formation ability (Figure 3A). The cell proliferation rates were also analyzed (Supplementary Figure 9). As predicted, depletion of TOP3 α abolished APB formation, while depletion of SUN1 in the TOP3 α -depleted cells led to recovered APB formation (Figure

3B, 3C). These results may imply that the detachment of telomeres from the nuclear envelope alleviates the requirement of TOP3 α to resolve topological stress.

Coil domain phosphorylation-mimetic mutations of RAP1 block the RAP1-SUN1 interaction

Since the detailed mechanism of the RAP1-SUN1 interaction is not fully understood, to determine which RAP1 domain interacts with SUN1, we generated various truncated forms of RAP1 for domain mapping (Figure 4A). The N-terminal domain of SUN1 is located in the nucleoplasm and interacts with RAP1, while the SUN1 C-terminus is located in the perinuclear space that anchors the protein to the nuclear envelope [47, 57]. Due to the difficulty of precipitating insoluble membrane proteins, we constructed a truncated form of SUN1 that contains 205 N-terminal soluble amino acids (SUN1 N205), which preserves the ability of SUN1 to interact with RAP1. U2OS cells were cotransfected with an HA-tagged RAP1 plasmid together with the EGFP-tagged SUN1 N205 plasmid to perform immunoprecipitation. Full-length HA-tagged RAP1 was efficiently coimmunoprecipitated with EGFP-tagged SUN1 N205 but not EGFP alone (Figure 4B). However, coil-deleted (Δ Coil) RAP1 was not coprecipitated with SUN1 (Figure 4B), suggesting that the coil region of RAP1 is critical for SUN1 binding.

Many protein-protein interactions are modulated through posttranslational modifications, such as phosphorylation. We were curious to know whether the interaction between human RAP1 and SUN1 may be regulated by RAP1 phosphorylation. We analyzed the potential phosphorylation of RAP1 using the proteomic PhosphoSitePlus[®] database (<https://www.phosphosite.org/homeAction.action>). There are 22 phosphorylation sites on RAP1, and eight phosphorylation sites are located within the coil region (Figure 4C). To characterize the kinases of these eight phosphorylation sites, the KinasePhos 2.0 website was used to predict the potential kinases (Table 1) [62]. Based on the analysis, S203, S205, S206, and S222 might be regulated by ATM kinase, Y195 and Y238 might be regulated by FGFR1, and T286 might be regulated by CK2. Next, we replaced these eight tyrosine, serine, or threonine residues with nonphosphorylatable phenylalanine and alanine (8FA) and phospho-mimetic aspartic acid and glutamic acid (8DE). Interestingly, the nonphosphorylatable RAP1-8FA mutations showed enhanced interactions with SUN1, but phospho-mimetic RAP1-8DE mutations lost the ability to interact with SUN1 (Figure 4D). These results suggest that this potential phosphorylation in the coil region of RAP1 might inhibit the interaction between RAP1 and SUN1.

RAP1-SUN1 interaction-independent nuclear envelope tethering pathways participate in APB formation

Finally, we investigated whether APB formation may be affected by the observed RAP1-SUN1 interaction. We simultaneously introduced RAP1-knockdown lentiviruses, which targeted the 3' UTR of RAP1, and knockdown-resistant RAP1-expressing lentiviruses into U2OS cells. We also deprived methionine in the medium to enrich the APB-positive subpopulations. The protein expression levels were determined by immunoblotting (Figure 5A). It has been reported that

the depletion of RAP1 hampers APB formation [33]. Consistent with this previous report, RAP1 knockdown in the U2OS cells led to decreased APB formation (Figure 5B). However, enforced expression of wild-type RAP1 to the endogenous level restored APB formation in the RAP1-depleted cells (Figure 5A, 5B). In addition, the cells expressing the RAP1 coil deletion and the nonphosphorylatable RAP1-8FA and phospho-mimetic RAP1-8DE mutants all displayed the same level of APBs, which was similar to that in the cells expressing wild-type RAP1 (Figure 5B). Our data imply that a SUN1-dependent but RAP1-independent pathway might contribute to APB formation in ALT cells.

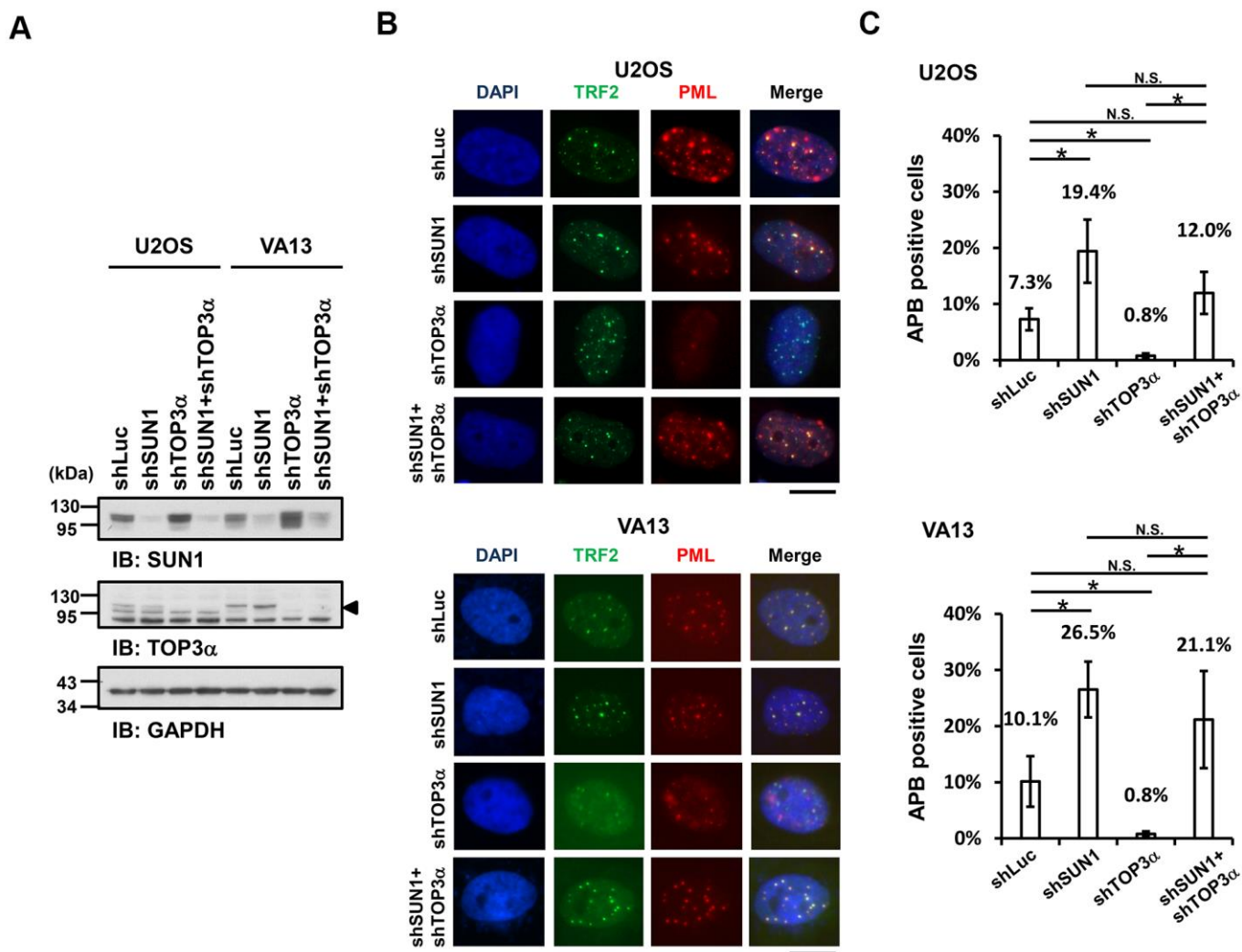


Figure 3. SUN1 depletion increases APB formation in TOP3 α -knockdown cells. (A) U2OS and VA13 cells were infected with control (shLuc), shSUN1, shTOP3 α , or shSUN1 combined with shTOP3 α lentiviruses and selected for 3 days. Cell lysates were analyzed by immunoblotting with anti-SUN1, anti-TOP3 α , and anti-GAPDH antibodies. The arrowhead indicates the location of the TOP3 α protein. GAPDH was used as the loading control. (B) Representative images show the colocalization of TRF2 and PML in U2OS cells (upper panel) and VA13 cells (bottom panel), as shown in Figure 1. Scale bar, 20 μ m. (C) Quantification of APBs (%) in the U2OS and VA13 cells shown in (B). Approximately 200-300 cells were analyzed for each independent experiment. Error bars denote SD; n=3 (independent experiments); *P<0.05 (two-tailed Student's t-test). N.S., no significance.

DISCUSSION

The first cytological evidence for telomere anchoring to the nuclear membrane was discovered by the Gasser laboratory [63]. In budding yeast, telomeres are clustered and placed at the nuclear periphery, where they create a nuclear subcompartment for telomere silencing [64]. It was reported that yeast subtelomeric Y' recombination is suppressed by telomere anchorage to the nuclear envelope [65]. Moreover, the yeast telomere-binding protein Rif1 is required for telomere anchorage [66]. In human telomerase-positive cells, telomere-nuclear envelope anchorage occurs during the cell cycle and is at least partly mediated through the

interaction between the shelterin subunit RAP1 and the nuclear envelope protein SUN1 [57]. Previous studies have also shown that in certain non-ALT cells, most telomeres are located within the nuclear interior during interphase [40, 67]. However, the telomere-nuclear envelope association in ALT cells had not been explored. Here, we show that SUN1 might play a role in preventing telomere-telomere recombination. We also reveal that potential phosphorylation at the RAP1 coil domain might decrease the interaction between RAP1 and SUN1. We hypothesize that with unknown environmental or internal stimuli, some unidentified kinases may phosphorylate the RAP1 coil domain to induce the dissolution of the RAP1 and SUN1

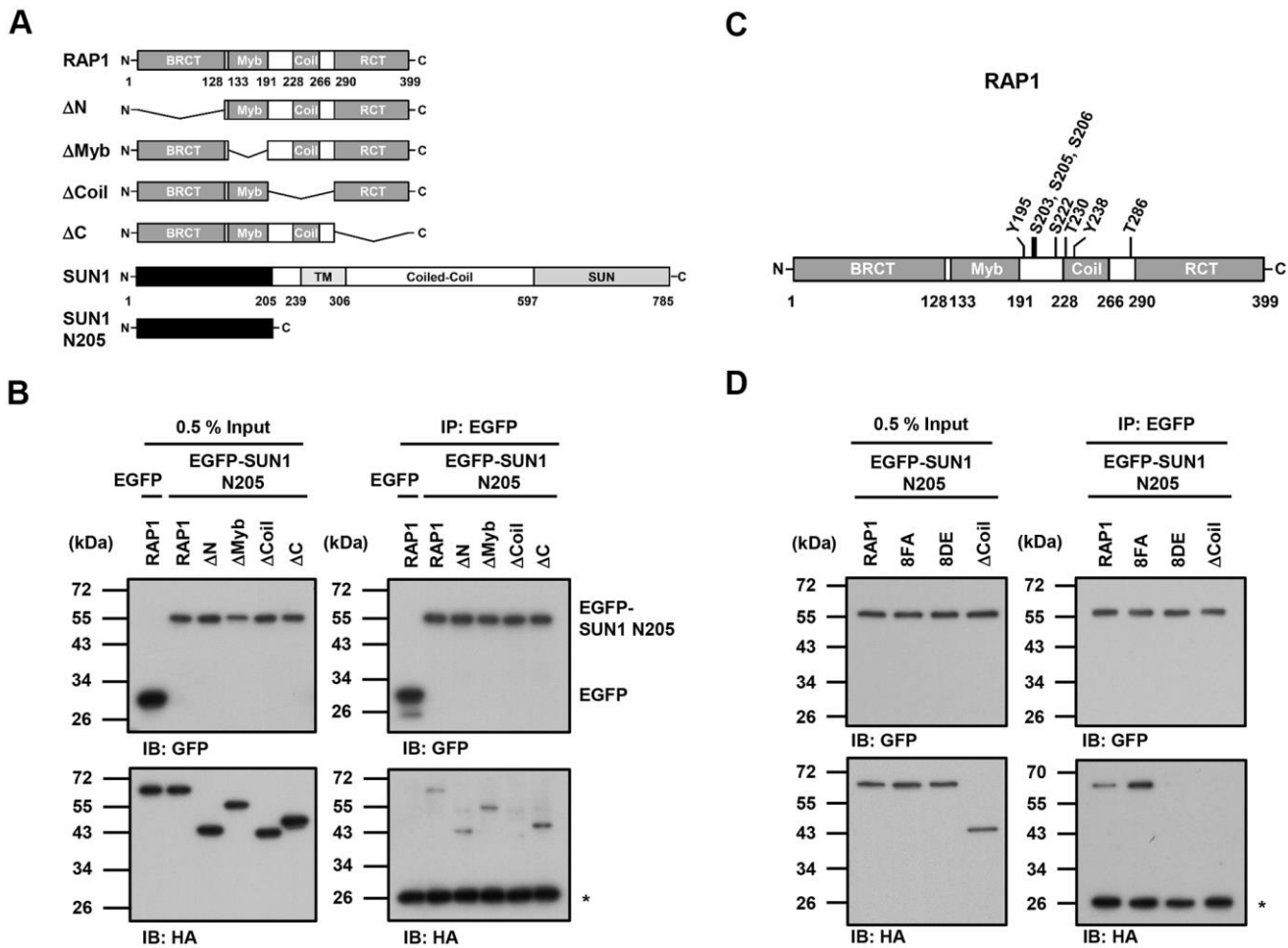


Figure 4. The coil region of RAP1 and the potential phosphorylation of residues in that domain are likely critical for the SUN1 interaction. (A) Schematic representations of the N-terminal HA-tagged RAP1 constructs and the N-terminal EGFP-tagged SUN1 constructs. TM, transmembrane. (B) U2OS cells were transfected with HA-tagged RAP1 together with either EGFP or EGFP-tagged SUN1 N205. Forty-eight hours posttransfection, the cells were harvested for use in immunoprecipitation assays. EGFP-SUN1 N205 was immunoprecipitated with anti-GFP beads. Input and immunoprecipitated proteins (IPs) were analyzed by immunoblotting with anti-GFP and anti-HA antibodies. Asterisk (*), nonspecific band. (C) A schematic representation of the eight potential phosphorylation sites in the coil domain of RAP1. (D) U2OS cells were transfected with HA-tagged RAP1 WT, nonphosphorylatable (8FA), or phospho-mimetic (8DE) mutant together with EGFP-tagged SUN1 N205. Forty-eight hours posttransfection, the cells were harvested for use in immunoprecipitation assays. Input and immunoprecipitated proteins (IPs) were analyzed by immunoblotting with anti-GFP and anti-HA antibodies. Asterisk (*), nonspecific band.

Table 1. Putative phosphorylation sites of RAP1 coil domain.

| Phosphorylation site | Sequence (N'→C') | Predicted kinase ^a | Score ^a | References |
|----------------------|------------------|-------------------------------|--------------------|------------|
| Y195 | 192 EHKYLLG | FGFR1 | 0.53 | |
| S203 | 220 APVSPSS | ATM | 0.93 | [87] |
| S205 | 202 VSPSSQK | ATM | 0.97 | [85] |
| S206 | 203 SPSSQKL | ATM | 0.93 | |
| S222 | 219 AADSGEP | ATM | 0.99 | |
| T230 | 227 NKRTPLD | GRK | 0.54 | |
| Y238 | 235 EEEYVKE | FGFR1 | 0.53 | |
| T286 | 283 DPPTPEE | CK2 | 0.59 | |

^aKinases were predicted and scored by KinasePhos2.0 (<http://kinasephos2.mbc.nctu.edu.tw/index.html>) [62].

interaction. The detailed mechanism of how telomeres leave the nuclear envelope and then generate APBs remains unclear (Figure 6A).

We observed that the APB formation is increased in SUN1-depleted ALT cells but is decreased in RAP1-SUN1 fusion ALT cells (Figure 6B). In budding and

fission yeasts, SUN1 homologs sequester double-strand breaks (DSBs) at the nuclear envelope to protect them from deleterious recombination [42, 43]. Based on these findings, one possible mechanism of SUN1-suppressed APB formation might be based on SUN1 sequestering telomeres to prevent their homologous recombination. Another plausible mechanism is that the SUN1-RAP1

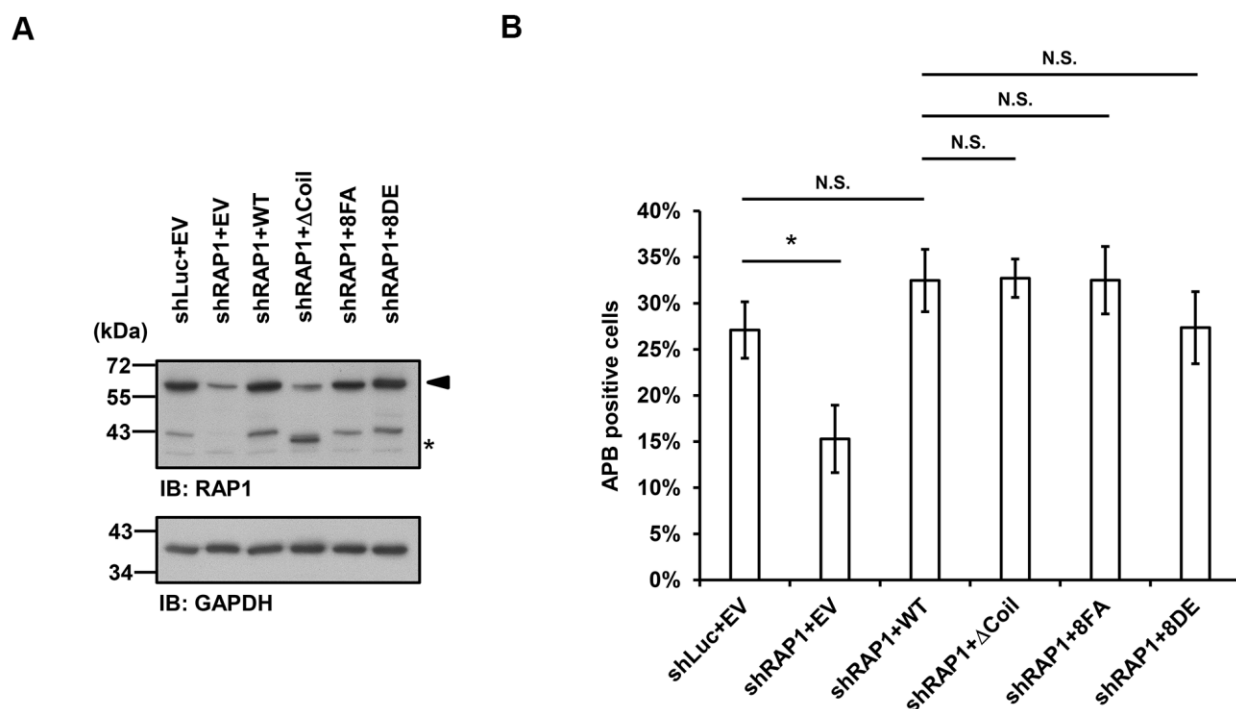


Figure 5. Disruption of the interaction between RAP1 and SUN1 does not interfere with APB formation in ALT cells. (A) U2OS cells were infected with the knockdown control (shLuc) or shRAP1 lentivirus and simultaneously complemented with control (EV), wild-type RAP1 (WT), RAP1 coil deletion (Δ Coil), nonphosphorylatable (8FA), or phospho-mimetic (8DE) RAP1 mutant lentiviruses. Virus-infected cells were selected for 5 days and subjected to further methionine restriction for 3 days. Cell lysates were analyzed by immunoblotting with anti-RAP1 and anti-GAPDH antibodies. The arrowhead indicates the location of endogenous RAP1, and the multiple lower-molecular-weight bands are degraded RAP1. Asterisk (*), RAP1 coil deletion mutant. GAPDH was used as the loading control. (B) Quantification of APBs (%) in the U2OS cells shown in (A). Approximately 200-300 cells were analyzed for each independent experiment. Error bars denote SD; n=3 (independent experiments); * $P < 0.05$ (two-tailed Student's t-test). N.S., no significance.

interaction may generate supercoiling tension that impedes subsequent telomere-telomere recombination. Crabbe and her colleagues revealed that not all telomeres are located in the nuclear interior during the cell cycle in telomerase-positive cells. In S phase, 25% of telomeres are located around the nuclear envelope. Furthermore, when entering the subsequent G1 stage, these cells retain approximately 40% of telomeres at the nuclear envelope [57]. We proposed that in SUN1-depleted ALT cells, the tethering force of telomeres on the nuclear envelope may partially loosen, which might provide more telomere flexibility and favor APB formation. In contrast, in RAP1-SUN1-expressing ALT cells, telomeres are forced “locked” with the nuclear envelope, which might enhance the difficulty of executing telomere-telomere recombination. Furthermore, ALT cells require TOP3 α to resolve topological stress caused by telomere-telomere recombination [60, 61]. We also found that knocking down SUN1 in TOP3 α -depleted ALT cells restored APB formation, which is consistent with the hypothesis that the topoisomerase activity of TOP3 α is dispensable in ALT cells when some telomeres are not tethered to the nucleus.

Telomere extension in ALT cells is mainly generated by the break-induced DNA replication (BIR) pathway [68–72]. Recently, it was discovered that ALT cells harbor bifurcated RAD52-dependent and RAD52-independent BIR pathways that lead to elongated telomeres. Both BIR pathways are involved in APB formations during ALT cell DNA synthesis, but only the RAD52-independent BIR pathway is critical for C-circle formation [18]. Telomeric DNA break-induced replication fork collapse and telomere damage-induced internal loops are both involved in C-circle formation [73, 74]. In SUN1-depleted cells, both the APB formation and C-circle levels were increased. Nevertheless, overexpression of the RAP1-SUN1 fusion protein constrains only APB formation but not C-circle levels. We speculate that ALT telomeric DNA might be more fragile to DNA replication fork-induced topological stress when the telomere ends are locked to the nuclear envelope. Subsequently, DNA replication fork collapse or DNA breakage might occur more frequently to induce C-circle formation.

Budding yeast contains two telomere-nuclear envelope anchoring pathways at different cell cycle stages. The

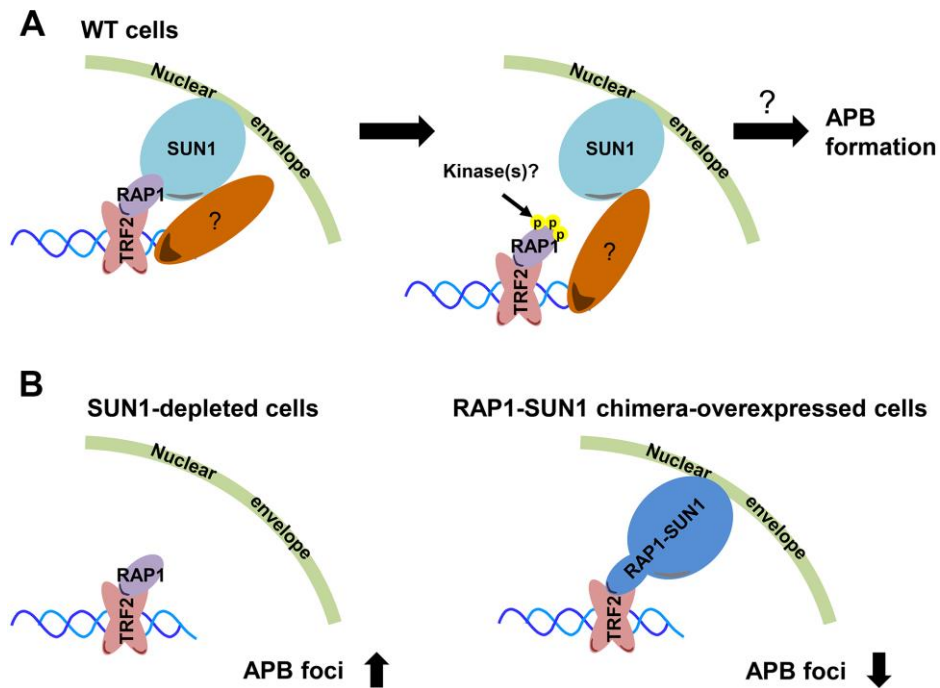


Figure 6. Model depicting the role of RAP1-SUN1-mediated telomere-nuclear envelope attachment during telomere-telomere recombination in ALT cells. (A) The interaction between RAP1 and SUN1 contributes to telomere anchorage to the nuclear envelope. Unknown kinases might phosphorylate the coil domain of RAP1, inducing RAP1 release from SUN1. Additionally, SUN1 might connect with an unknown telomere-binding protein, and this interaction may provide another telomere-nuclear envelope tethering mechanism to constrain the telomere from freely roaming. The molecular mechanism of how the telomeres depart from the nuclear envelope to the APB remains a mystery. **(B)** The depletion of SUN1 leads to the release telomeres from the nuclear envelope anchorage and increases the APB formation. However, the RAP1-SUN1 chimera enforces anchorage and decreases the APB formation in ALT cells.

telomere-associated proteins Sir4 and yKu contact the nuclear inner membrane proteins Mps3 and Esc1, respectively, at different cell cycle stages [75]. In mammals, while telomeres can be tethered to the nuclear envelope via the RAP1-SUN1 interaction, cells with RAP1 depletion still retain approximately 40% of telomeres at the nuclear periphery after mitosis [57]. Here, we found that RAP1 interacts with SUN1 in the nucleoplasm via its coil region, and the phospho-mimetic mutant impedes the RAP1-SUN1 interaction. However, complementing RAP1-depleted cells with the RAP1 coil deletion or phosphoryl-mimetic mutant did not increase the APB formation. Considering this discrepancy, we hypothesize that another nuclear tethering force might influence APB formation. SUN1 might simultaneously bind another telomeric protein (Figure 6A). Another possibility is that another tethering mechanism bridges telomeres to the nuclear envelope. These possibilities might explain why we could not specifically detect the contribution of the RAP1-SUN1 interaction to APB formation. Cho and his colleagues found that homology searching and directional telomere movement in ALT cells is based on a meiosis-specific complex to perform nonsister homologous chromatid repair [76]. Moreover, in the mammalian meiotic cell cycle, a RAP1-independent telomere-nuclear envelope tethering pathway indeed exists [77]. The nuclear envelope protein complex TERB1/2-MAJIN provides alternative telomere-nuclear membrane attachment during meiosis, suggesting that the telomere-TERB1-TERB2-MAJIN-nuclear envelope associating with the telomere-LINC complex may cooperatively recruit telomeres to the nuclear envelope during meiosis [78, 79]. Recent studies have shown that SUN1 interacts with MAJIN and TERB1 [80, 81]. Therefore, a possible explanation is that ALT cells might borrow meiotic proteins, such as the TERB1/2-MAJIN complex, to orchestrate telomere attachment during the mitotic cell cycle.

In the fission yeast *Schizosaccharomyces pombe*, telomeres are tethered to the nuclear envelope in interphase via the interaction between Rap1 (a homolog of human RAP1) and the inner nuclear membrane protein Bqt4, which connects telomeres to the nuclear envelope during both vegetative growth and meiosis [82]. The dissociation of Rap1 from Bqt4 is promoted by CDK-mediated Rap1 hyperphosphorylation at the early M phase, which is required for faithful chromosomal segregation [83]. In fact, in contrast to the “closed mitosis” of *S. pombe*, higher eukaryotes usually undergo nuclear envelope breakdown to release their chromosomes from the nuclear envelope [5]. Although human RAP1 phosphorylation may repress the RAP1-SUN1 interaction, the molecular details of this process in ALT cells remain to be elucidated in further investigations.

This study revealed that telomere-nuclear envelope anchorage interferes with the telomere-telomere recombination pathway in ALT cells. Incomplete telomere detachment from the nuclear envelope may cause the dysregulation of chromatin dynamics. As cell cycle checkpoint pathways, the maintenance of the homeostasis between the nuclear envelope and telomeres may be tightly regulated and important for cell cycle progression. Interestingly, a recent study showed that the mislocalization of LINC complex proteins is a significant characteristic of cellular senescence [84]. Notably, RAP1 S205 phosphorylation, which is activated by p90RS activation, induces the nuclear export of the RAP1-TRF2 complex and further contributes to senescence and telomere dysfunction in epithelial cells [85, 86]. When telomeres are shortened, the ALT pathway is induced by complicated DNA damage signaling and (epi)genetic modification aberrations [22]. Therefore, the correlation between the LINC complex and RAP1 phosphorylation in the progression of senescence and how homeostasis between telomeres and the nuclear envelope is maintained will be important issues for further determination.

Abbreviations

ALT: alternative lengthening of telomeres; PML: promyelocytic leukemia protein; APBs: ALT-associated PML bodies; T-SCE: telomeric sister chromatid exchange; MEF: mouse embryonic fibroblast; LINC: linkers of nucleoskeleton and cytoskeleton; shRNA: short hairpin RNA; SD: standard deviation; TRF: telomere restriction fragment; RCT: RAP1 C terminal; SUN1 N205: a truncated form of SUN1 that contains 205 N-terminal soluble amino acids; DSB: double-strand break; BIR: break-induced DNA replication.

AUTHOR CONTRIBUTIONS

S.-C.T. conceived and designed the experiments; C.-W.Y., M.-H.H., and H.-J.S. performed the experiments; and S.-C.T. wrote the paper with the help of C.-W.Y.

ACKNOWLEDGMENTS

We thank Drs. Angelika A. Noegel (University of Cologne), Tsai-Kun Li (National Taiwan University), and Jan Karlseder (Salk Institute) for kindly providing plasmids and cell lines.

CONFLICTS OF INTEREST

The authors declare that they have no conflicts of interest.

FUNDING

This work was supported by the “Center of Precision Medicine” from The Featured Areas Research Center Program within the framework of the Higher Education Sprout Project by the Ministry of Education (MOE) and the National Health Research Institutes (NHRI) [NHRI-EX108-10825BI] to Shu-Chun Teng.

REFERENCES

1. Blackburn EH, Epel ES, Lin J. Human telomere biology: A contributory and interactive factor in aging, disease risks, and protection. *Science*. 2015; 350:1193–98. <https://doi.org/10.1126/science.aab3389> PMID:[26785477](https://pubmed.ncbi.nlm.nih.gov/26785477/)
2. de Lange T. Protection of mammalian telomeres. *Oncogene*. 2002; 21:532–40. <https://doi.org/10.1038/sj.onc.1205080> PMID:[11850778](https://pubmed.ncbi.nlm.nih.gov/11850778/)
3. Greider CW, Blackburn EH. Identification of a specific telomere terminal transferase activity in Tetrahymena extracts. *Cell*. 1985; 43:405–13. [https://doi.org/10.1016/0092-8674\(85\)90170-9](https://doi.org/10.1016/0092-8674(85)90170-9) PMID:[3907856](https://pubmed.ncbi.nlm.nih.gov/3907856/)
4. Artandi SE, DePinho RA. A critical role for telomeres in suppressing and facilitating carcinogenesis. *Curr Opin Genet Dev*. 2000; 10:39–46. [https://doi.org/10.1016/S0959-437X\(99\)00047-7](https://doi.org/10.1016/S0959-437X(99)00047-7) PMID:[10679392](https://pubmed.ncbi.nlm.nih.gov/10679392/)
5. Hetzer MW, Walther TC, Mattaj IW. Pushing the envelope: structure, function, and dynamics of the nuclear periphery. *Annu Rev Cell Dev Biol*. 2005; 21:347–80. <https://doi.org/10.1146/annurev.cellbio.21.090704.151152> PMID:[16212499](https://pubmed.ncbi.nlm.nih.gov/16212499/)
6. Cesare AJ, Reddel RR. Alternative lengthening of telomeres: models, mechanisms and implications. *Nat Rev Genet*. 2010; 11:319–30. <https://doi.org/10.1038/nrg2763> PMID:[20351727](https://pubmed.ncbi.nlm.nih.gov/20351727/)
7. Bryan TM, Englezou A, Dalla-Pozza L, Dunham MA, Reddel RR. Evidence for an alternative mechanism for maintaining telomere length in human tumors and tumor-derived cell lines. *Nat Med*. 1997; 3:1271–74. <https://doi.org/10.1038/nm1197-1271> PMID:[9359704](https://pubmed.ncbi.nlm.nih.gov/9359704/)
8. Bryan TM, Englezou A, Gupta J, Bacchetti S, Reddel RR. Telomere elongation in immortal human cells without detectable telomerase activity. *EMBO J*. 1995; 14:4240–48. PMID:[7556065](https://pubmed.ncbi.nlm.nih.gov/7556065/)
9. Sobinoff AP, Pickett HA. Alternative lengthening of telomeres: DNA repair pathways converge. *Trends Genet*. 2017; 33:921–32. <https://doi.org/10.1016/j.tig.2017.09.003> PMID:[28969871](https://pubmed.ncbi.nlm.nih.gov/28969871/)
10. Yeager TR, Neumann AA, Englezou A, Huschtscha LI, Noble JR, Reddel RR. Telomerase-negative immortalized human cells contain a novel type of promyelocytic leukemia (PML) body. *Cancer Res*. 1999; 59:4175–79. PMID:[10485449](https://pubmed.ncbi.nlm.nih.gov/10485449/)
11. Acharya S, Kaul Z, Gocha AS, Martinez AR, Harris J, Parvin JD, Groden J. Association of BLM and BRCA1 during telomere maintenance in ALT cells. *PLoS One*. 2014; 9:e103819. <https://doi.org/10.1371/journal.pone.0103819> PMID:[25084169](https://pubmed.ncbi.nlm.nih.gov/25084169/)
12. Lillard-Wetherell K, Machwe A, Langland GT, Combs KA, Behbehani GK, Schonberg SA, German J, Turchi JJ, Orren DK, Groden J. Association and regulation of the BLM helicase by the telomere proteins TRF1 and TRF2. *Hum Mol Genet*. 2004; 13:1919–32. <https://doi.org/10.1093/hmg/ddh193> PMID:[15229185](https://pubmed.ncbi.nlm.nih.gov/15229185/)
13. Nabetani A, Yokoyama O, Ishikawa F. Localization of hRad9, hHus1, hRad1, and hRad17 and caffeine-sensitive DNA replication at the alternative lengthening of telomeres-associated promyelocytic leukemia body. *J Biol Chem*. 2004; 279:25849–57. <https://doi.org/10.1074/jbc.M312652200> PMID:[15075340](https://pubmed.ncbi.nlm.nih.gov/15075340/)
14. O’Sullivan RJ, Arnoult N, Lackner DH, Oganessian L, Haggblom C, Corpet A, Almouzni G, Karlseder J. Rapid induction of alternative lengthening of telomeres by depletion of the histone chaperone ASF1. *Nat Struct Mol Biol*. 2014; 21:167–74. <https://doi.org/10.1038/nsmb.2754> PMID:[24413054](https://pubmed.ncbi.nlm.nih.gov/24413054/)
15. Potts PR, Yu H. The SMC5/6 complex maintains telomere length in ALT cancer cells through SUMOylation of telomere-binding proteins. *Nat Struct Mol Biol*. 2007; 14:581–90. <https://doi.org/10.1038/nsmb1259> PMID:[17589526](https://pubmed.ncbi.nlm.nih.gov/17589526/)
16. Stavropoulos DJ, Bradshaw PS, Li X, Pasic I, Truong K, Ikura M, Ungrin M, Meyn MS. The Bloom syndrome helicase BLM interacts with TRF2 in ALT cells and promotes telomeric DNA synthesis. *Hum Mol Genet*. 2002; 11:3135–44. <https://doi.org/10.1093/hmg/11.25.3135> PMID:[12444098](https://pubmed.ncbi.nlm.nih.gov/12444098/)
17. Wu G, Lee WH, Chen PL. NBS1 and TRF1 colocalize at promyelocytic leukemia bodies during late S/G2 phases in immortalized telomerase-negative cells.

- Implication of NBS1 in alternative lengthening of telomeres. *J Biol Chem.* 2000; 275:30618–22.
<https://doi.org/10.1074/jbc.C000390200>
 PMID:10913111
18. Zhang JM, Yadav T, Ouyang J, Lan L, Zou L. Alternative lengthening of telomeres through two distinct break-induced replication pathways. *Cell Rep.* 2019; 26:955–68.e3.
<https://doi.org/10.1016/j.celrep.2018.12.102>
 PMID:30673617
 19. Molenaar C, Wiesmeijer K, Verwoerd NP, Khazen S, Eils R, Tanke HJ, Dirks RW. Visualizing telomere dynamics in living mammalian cells using PNA probes. *EMBO J.* 2003; 22:6631–41.
<https://doi.org/10.1093/emboj/cdg633>
 PMID:14657034
 20. Grobelny JV, Godwin AK, Broccoli D. ALT-associated PML bodies are present in viable cells and are enriched in cells in the G(2)/M phase of the cell cycle. *J Cell Sci.* 2000; 113:4577–85.
 PMID:11082050
 21. Jegou T, Chung I, Heuvelman G, Wachsmuth M, Görisch SM, Greulich-Bode KM, Boukamp P, Lichter P, Rippe K. Dynamics of telomeres and promyelocytic leukemia nuclear bodies in a telomerase-negative human cell line. *Mol Biol Cell.* 2009; 20:2070–82.
<https://doi.org/10.1091/mbc.e08-02-0108>
 PMID:19211845
 22. Chung I, Osterwald S, Deeg KI, Rippe K. PML body meets telomere: the beginning of an ALternate ending? *Nucleus.* 2012; 3:263–75.
<https://doi.org/10.4161/nucl.20326> PMID:22572954
 23. Draskovic I, Arnoult N, Steiner V, Bacchetti S, Lomonte P, Londoño-Vallejo A. Probing PML body function in ALT cells reveals spatiotemporal requirements for telomere recombination. *Proc Natl Acad Sci USA.* 2009; 106:15726–31.
<https://doi.org/10.1073/pnas.0907689106>
 PMID:19717459
 24. Cesare AJ, Griffith JD. Telomeric DNA in ALT cells is characterized by free telomeric circles and heterogeneous t-loops. *Mol Cell Biol.* 2004; 24:9948–57.
<https://doi.org/10.1128/MCB.24.22.9948-9957.2004>
 PMID:15509797
 25. Henson JD, Cao Y, Huschtscha LI, Chang AC, Au AY, Pickett HA, Reddel RR. DNA C-circles are specific and quantifiable markers of alternative-lengthening-of-telomeres activity. *Nat Biotechnol.* 2009; 27:1181–85.
<https://doi.org/10.1038/nbt.1587> PMID:19935656
 26. Henson JD, Lau LM, Koch S, Martin La Rotta N, Dagg RA, Reddel RR. The C-Circle Assay for alternative-lengthening-of-telomeres activity. *Methods.* 2017; 114:74–84.
<https://doi.org/10.1016/j.ymeth.2016.08.016>
 PMID:27595911
 27. Nabetani A, Ishikawa F. Unusual telomeric DNAs in human telomerase-negative immortalized cells. *Mol Cell Biol.* 2009; 29:703–13.
<https://doi.org/10.1128/MCB.00603-08>
 PMID:19015236
 28. Ogino H, Nakabayashi K, Suzuki M, Takahashi E, Fujii M, Suzuki T, Ayusawa D. Release of telomeric DNA from chromosomes in immortal human cells lacking telomerase activity. *Biochem Biophys Res Commun.* 1998; 248:223–27.
<https://doi.org/10.1006/bbrc.1998.8875>
 PMID:9675117
 29. Tokutake Y, Matsumoto T, Watanabe T, Maeda S, Tahara H, Sakamoto S, Niida H, Sugimoto M, Ide T, Furuichi Y. Extra-chromosomal telomere repeat DNA in telomerase-negative immortalized cell lines. *Biochem Biophys Res Commun.* 1998; 247:765–72.
<https://doi.org/10.1006/bbrc.1998.8876>
 PMID:9647768
 30. Wang RC, Smogorzewska A, de Lange T. Homologous recombination generates T-loop-sized deletions at human telomeres. *Cell.* 2004; 119:355–68.
<https://doi.org/10.1016/j.cell.2004.10.011>
 PMID:15507207
 31. de Lange T. Shelterin: the protein complex that shapes and safeguards human telomeres. *Genes Dev.* 2005; 19:2100–10.
<https://doi.org/10.1101/gad.1346005> PMID:16166375
 32. Wu G, Jiang X, Lee WH, Chen PL. Assembly of functional ALT-associated promyelocytic leukemia bodies requires Nijmegen Breakage Syndrome 1. *Cancer Res.* 2003; 63:2589–95.
 PMID:12750284
 33. Jiang WQ, Zhong ZH, Henson JD, Reddel RR. Identification of candidate alternative lengthening of telomeres genes by methionine restriction and RNA interference. *Oncogene.* 2007; 26:4635–47.
<https://doi.org/10.1038/sj.onc.1210260>
 PMID:17297460
 34. Martinez P, Thanasoula M, Carlos AR, Gómez-López G, Tejera AM, Schoeftner S, Dominguez O, Pisano DG, Tarsounas M, Blasco MA. Mammalian Rap1 controls telomere function and gene expression through binding to telomeric and extratelomeric sites. *Nat Cell Biol.* 2010; 12:768–80.
<https://doi.org/10.1038/ncb2081> PMID:20622869
 35. Sfeir A, Kabir S, van Overbeek M, Celli GB, de Lange T. Loss of Rap1 induces telomere recombination in the

- absence of NHEJ or a DNA damage signal. *Science*. 2010; 327:1657–61.
<https://doi.org/10.1126/science.1185100>
PMID:20339076
36. Crisp M, Liu Q, Roux K, Rattner JB, Shanahan C, Burke B, Stahl PD, Hodzic D. Coupling of the nucleus and cytoplasm: role of the LINC complex. *J Cell Biol*. 2006; 172:41–53.
<https://doi.org/10.1083/jcb.200509124>
PMID:16380439
37. Padmakumar VC, Libotte T, Lu W, Zaim H, Abraham S, Noegel AA, Gotzmann J, Foisner R, Karakesiosoglou I. The inner nuclear membrane protein Sun1 mediates the anchorage of Nesprin-2 to the nuclear envelope. *J Cell Sci*. 2005; 118:3419–30.
<https://doi.org/10.1242/jcs.02471> PMID:16079285
38. Chang W, Worman HJ, Gundersen GG. Accessorizing and anchoring the LINC complex for multifunctionality. *J Cell Biol*. 2015; 208:11–22.
<https://doi.org/10.1083/jcb.201409047>
PMID:25559183
39. Aymard F, Aguirrebengoa M, Guillou E, Javierre BM, Bugler B, Arnould C, Rocher V, Iacovoni JS, Biernacka A, Skrzypczak M, Ginalski K, Rowicka M, Fraser P, Legube G. Genome-wide mapping of long-range contacts unveils clustering of DNA double-strand breaks at damaged active genes. *Nat Struct Mol Biol*. 2017; 24:353–61.
<https://doi.org/10.1038/nsmb.3387> PMID:28263325
40. Lottersberger F, Karssemeijer RA, Dimitrova N, de Lange T. 53BP1 and the LINC complex promote microtubule-dependent DSB mobility and DNA repair. *Cell*. 2015; 163:880–93.
<https://doi.org/10.1016/j.cell.2015.09.057>
PMID:26544937
41. Marnef A, Finoux AL, Arnould C, Guillou E, Daburon V, Rocher V, Mangeat T, Mangeot PE, Ricci EP, Legube G. A cohesin/HUSH- and LINC-dependent pathway controls ribosomal DNA double-strand break repair. *Genes Dev*. 2019; 33:1175–90.
<https://doi.org/10.1101/gad.324012.119>
PMID:31395742
42. Oza P, Jaspersen SL, Miele A, Dekker J, Peterson CL. Mechanisms that regulate localization of a DNA double-strand break to the nuclear periphery. *Genes Dev*. 2009; 23:912–27.
<https://doi.org/10.1101/gad.1782209> PMID:19390086
43. Swartz RK, Rodriguez EC, King MC. A role for nuclear envelope-bridging complexes in homology-directed repair. *Mol Biol Cell*. 2014; 25:2461–71.
<https://doi.org/10.1091/mbc.e13-10-0569>
PMID:24943839
44. Malone CJ, Fixsen WD, Horvitz HR, Han M. UNC-84 localizes to the nuclear envelope and is required for nuclear migration and anchoring during *C. elegans* development. *Development*. 1999; 126:3171–81.
PMID:10375507
45. Starr DA, Han M. Role of ANC-1 in tethering nuclei to the actin cytoskeleton. *Science*. 2002; 298:406–09.
<https://doi.org/10.1126/science.1075119>
PMID:12169658
46. Starr DA, Hermann GJ, Malone CJ, Fixsen W, Priess JR, Horvitz HR, Han M. unc-83 encodes a novel component of the nuclear envelope and is essential for proper nuclear migration. *Development*. 2001; 128:5039–50.
PMID:11748140
47. Haque F, Lloyd DJ, Smallwood DT, Dent CL, Shanahan CM, Fry AM, Trembath RC, Shackleton S. SUN1 interacts with nuclear lamin A and cytoplasmic nesprins to provide a physical connection between the nuclear lamina and the cytoskeleton. *Mol Cell Biol*. 2006; 26:3738–51.
<https://doi.org/10.1128/MCB.26.10.3738-3751.2006>
PMID:16648470
48. Matsumoto A, Hieda M, Yokoyama Y, Nishioka Y, Yoshidome K, Tsujimoto M, Matsuura N. Global loss of a nuclear lamina component, lamin A/C, and LINC complex components SUN1, SUN2, and nesprin-2 in breast cancer. *Cancer Med*. 2015; 4:1547–57.
<https://doi.org/10.1002/cam4.495> PMID:26175118
49. Horn HF, Kim DI, Wright GD, Wong ES, Stewart CL, Burke B, Roux KJ. A mammalian KASH domain protein coupling meiotic chromosomes to the cytoskeleton. *J Cell Biol*. 2013; 202:1023–39.
<https://doi.org/10.1083/jcb.201304004>
PMID:24062341
50. Li P, Noegel AA. Inner nuclear envelope protein SUN1 plays a prominent role in mammalian mRNA export. *Nucleic Acids Res*. 2015; 43:9874–88.
<https://doi.org/10.1093/nar/gkv1058> PMID:26476453
51. Liu Q, Pante N, Misteli T, Elsagga M, Crisp M, Hodzic D, Burke B, Roux KJ. Functional association of Sun1 with nuclear pore complexes. *J Cell Biol*. 2007; 178:785–98.
<https://doi.org/10.1083/jcb.200704108>
PMID:17724119
52. Talamas JA, Hetzer MW. POM121 and Sun1 play a role in early steps of interphase NPC assembly. *J Cell Biol*. 2011; 194:27–37.
<https://doi.org/10.1083/jcb.201012154>
PMID:21727197
53. Ferguson M, Ward DC. Cell cycle dependent chromosomal movement in pre-mitotic human T-lymphocyte nuclei. *Chromosoma*. 1992; 101:557–65.
<https://doi.org/10.1007/BF00660315> PMID:1521500

54. de Lange T. Human telomeres are attached to the nuclear matrix. *EMBO J.* 1992; 11:717–24. PMID:[1537344](https://pubmed.ncbi.nlm.nih.gov/1537344/)
55. Ludérus ME, van Steensel B, Chong L, Sibon OC, Cremers FF, de Lange T. Structure, subnuclear distribution, and nuclear matrix association of the mammalian telomeric complex. *J Cell Biol.* 1996; 135:867–81. <https://doi.org/10.1083/jcb.135.4.867> PMID:[8922373](https://pubmed.ncbi.nlm.nih.gov/8922373/)
56. Weipoltshammer K, Schöfer C, Almeder M, Philimonenko VV, Frei K, Wachtler F, Hozák P. Intracellular anchoring of repetitive DNA sequences: centromeres, telomeres, and ribosomal DNA. *J Cell Biol.* 1999; 147:1409–18. <https://doi.org/10.1083/jcb.147.7.1409> PMID:[10613900](https://pubmed.ncbi.nlm.nih.gov/10613900/)
57. Crabbe L, Cesare AJ, Kasuboski JM, Fitzpatrick JA, Karlseder J. Human telomeres are tethered to the nuclear envelope during postmitotic nuclear assembly. *Cell Rep.* 2012; 2:1521–29. <https://doi.org/10.1016/j.celrep.2012.11.019> PMID:[23260663](https://pubmed.ncbi.nlm.nih.gov/23260663/)
58. Li B, Oestreich S, de Lange T. Identification of human Rap1: implications for telomere evolution. *Cell.* 2000; 101:471–83. [https://doi.org/10.1016/S0092-8674\(00\)80858-2](https://doi.org/10.1016/S0092-8674(00)80858-2) PMID:[10850490](https://pubmed.ncbi.nlm.nih.gov/10850490/)
59. Flynn RL, Cox KE, Jeitany M, Wakimoto H, Bryll AR, Ganem NJ, Bersani F, Pineda JR, Suvà ML, Benes CH, Haber DA, Boussin FD, Zou L. Alternative lengthening of telomeres renders cancer cells hypersensitive to ATR inhibitors. *Science.* 2015; 347:273–77. <https://doi.org/10.1126/science.1257216> PMID:[25593184](https://pubmed.ncbi.nlm.nih.gov/25593184/)
60. Tsai HJ, Huang WH, Li TK, Tsai YL, Wu KJ, Tseng SF, Teng SC. Involvement of topoisomerase III in telomere-telomere recombination. *J Biol Chem.* 2006; 281:13717–23. <https://doi.org/10.1074/jbc.M600649200> PMID:[16546998](https://pubmed.ncbi.nlm.nih.gov/16546998/)
61. Temime-Smaali N, Guittat L, Wenner T, Bayart E, Douarre C, Gomez D, Giraud-Panis MJ, Londono-Vallejo A, Gilson E, Amor-Guérét M, Riou JF. Topoisomerase III α is required for normal proliferation and telomere stability in alternative lengthening of telomeres. *EMBO J.* 2008; 27:1513–24. <https://doi.org/10.1038/emboj.2008.74> PMID:[18418389](https://pubmed.ncbi.nlm.nih.gov/18418389/)
62. Wong YH, Lee TY, Liang HK, Huang CM, Wang TY, Yang YH, Chu CH, Huang HD, Ko MT, Hwang JK. KinasePhos 2.0: a web server for identifying protein kinase-specific phosphorylation sites based on sequences and coupling patterns. *Nucleic Acids Res.* 2007 (Suppl 2); 35:W588-94. <https://doi.org/10.1093/nar/gkm322> PMID:[17517770](https://pubmed.ncbi.nlm.nih.gov/17517770/)
63. Gotta M, Laroche T, Formenton A, Maillet L, Scherthan H, Gasser SM. The clustering of telomeres and colocalization with Rap1, Sir3, and Sir4 proteins in wild-type *Saccharomyces cerevisiae*. *J Cell Biol.* 1996; 134:1349–63. <https://doi.org/10.1083/jcb.134.6.1349> PMID:[8830766](https://pubmed.ncbi.nlm.nih.gov/8830766/)
64. Hediger F, Neumann FR, Van Houwe G, Dubrana K, Gasser SM. Live imaging of telomeres: γ Ku and Sir proteins define redundant telomere-anchoring pathways in yeast. *Curr Biol.* 2002; 12:2076–89. [https://doi.org/10.1016/S0960-9822\(02\)01338-6](https://doi.org/10.1016/S0960-9822(02)01338-6) PMID:[12498682](https://pubmed.ncbi.nlm.nih.gov/12498682/)
65. Schober H, Ferreira H, Kalck V, Gehlen LR, Gasser SM. Yeast telomerase and the SUN domain protein Mps3 anchor telomeres and repress subtelomeric recombination. *Genes Dev.* 2009; 23:928–38. <https://doi.org/10.1101/gad.1787509> PMID:[19390087](https://pubmed.ncbi.nlm.nih.gov/19390087/)
66. Park S, Patterson EE, Cobb J, Audhya A, Gartenberg MR, Fox CA. Palmitoylation controls the dynamics of budding-yeast heterochromatin via the telomere-binding protein Rif1. *Proc Natl Acad Sci USA.* 2011; 108:14572–77. <https://doi.org/10.1073/pnas.1105262108> PMID:[21844336](https://pubmed.ncbi.nlm.nih.gov/21844336/)
67. van Koningsbruggen S, Gierlinski M, Schofield P, Martin D, Barton GJ, Ariyurek Y, den Dunnen JT, Lamond AI. High-resolution whole-genome sequencing reveals that specific chromatin domains from most human chromosomes associate with nucleoli. *Mol Biol Cell.* 2010; 21:3735–48. <https://doi.org/10.1091/mbc.e10-06-0508> PMID:[20826608](https://pubmed.ncbi.nlm.nih.gov/20826608/)
68. Dunham MA, Neumann AA, Fasching CL, Reddel RR. Telomere maintenance by recombination in human cells. *Nat Genet.* 2000; 26:447–50. <https://doi.org/10.1038/82586> PMID:[11101843](https://pubmed.ncbi.nlm.nih.gov/11101843/)
69. Sobinoff AP, Allen JA, Neumann AA, Yang SF, Walsh ME, Henson JD, Reddel RR, Pickett HA. BLM and SLX4 play opposing roles in recombination-dependent replication at human telomeres. *EMBO J.* 2017; 36:2907–19. <https://doi.org/10.15252/emboj.201796889> PMID:[28877996](https://pubmed.ncbi.nlm.nih.gov/28877996/)
70. Roumelioti FM, Sotiriou SK, Katsini V, Chiourea M, Halazonetis TD, Gagos S. Alternative lengthening of human telomeres is a conservative DNA replication

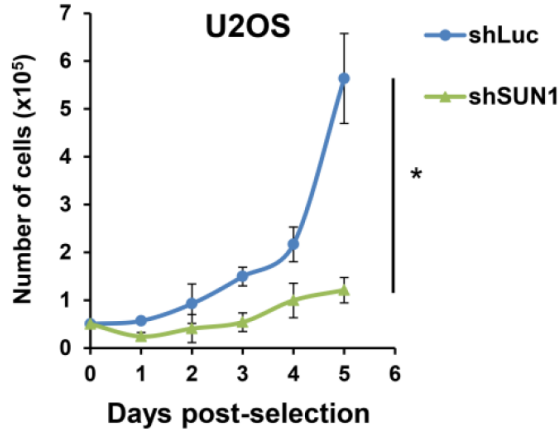
- process with features of break-induced replication. *EMBO Rep.* 2016; 17:1731–37.
<https://doi.org/10.15252/embr.201643169>
 PMID:27760777
71. Min J, Wright WE, Shay JW. Alternative lengthening of telomeres mediated by mitotic DNA synthesis engages break-induced replication processes. *Mol Cell Biol.* 2017; 37:e00226–17.
<https://doi.org/10.1128/MCB.00226-17>
 PMID:28760773
72. Özer Ö, Bhowmick R, Liu Y, Hickson ID. Human cancer cells utilize mitotic DNA synthesis to resist replication stress at telomeres regardless of their telomere maintenance mechanism. *Oncotarget.* 2018; 9:15836–46.
<https://doi.org/10.18632/oncotarget.24745>
 PMID:29662610
73. Mazzucco G, Huda A, Galli M, Piccini D, Giannattasio M, Pessina F, Doksan Y. Telomere damage induces internal loops that generate telomeric circles. *Nat Commun.* 2020; 11:5297.
<https://doi.org/10.1038/s41467-020-19139-4>
 PMID:33082350
74. Zhang T, Zhang Z, Shengzhao G, Li X, Liu H, Zhao Y. Strand break-induced replication fork collapse leads to C-circles, C-overhangs and telomeric recombination. *PLoS Genet.* 2019; 15:e1007925.
<https://doi.org/10.1371/journal.pgen.1007925>
 PMID:30716077
75. Taddei A, Gasser SM. Structure and function in the budding yeast nucleus. *Genetics.* 2012; 192:107–29.
<https://doi.org/10.1534/genetics.112.140608>
 PMID:22964839
76. Cho NW, Dilley RL, Lampson MA, Greenberg RA. Interchromosomal homology searches drive directional ALT telomere movement and synapsis. *Cell.* 2014; 159:108–21.
<https://doi.org/10.1016/j.cell.2014.08.030>
 PMID:25259924
77. Scherthan H, Sfeir A, de Lange T. Rap1-independent telomere attachment and bouquet formation in mammalian meiosis. *Chromosoma.* 2011; 120:151–57.
<https://doi.org/10.1007/s00412-010-0295-4>
 PMID:20927532
78. Shibuya H, Hernández-Hernández A, Morimoto A, Negishi L, Höög C, Watanabe Y. MAJIN links telomeric DNA to the nuclear membrane by exchanging telomere cap. *Cell.* 2015; 163:1252–66.
<https://doi.org/10.1016/j.cell.2015.10.030>
 PMID:26548954
79. Wang Y, Chen Y, Chen J, Wang L, Nie L, Long J, Chang H, Wu J, Huang C, Lei M. The meiotic TERB1-TERB2-MAJIN complex tethers telomeres to the nuclear envelope. *Nat Commun.* 2019; 10:564.
<https://doi.org/10.1038/s41467-019-08437-1>
 PMID:30718482
80. Wang G, Wu X, Zhou L, Gao S, Yun D, Liang A, Sun F. Tethering of telomeres to the nuclear envelope is mediated by SUN1-MAJIN and possibly promoted by SPDYA-CDK2 during meiosis. *Front Cell Dev Biol.* 2020; 8:845.
<https://doi.org/10.3389/fcell.2020.00845>
 PMID:33015044
81. Shibuya H, Ishiguro K, Watanabe Y. The TRF1-binding protein TERB1 promotes chromosome movement and telomere rigidity in meiosis. *Nat Cell Biol.* 2014; 16:145–56.
<https://doi.org/10.1038/ncb2896>
 PMID:24413433
82. Chikashige Y, Yamane M, Okamasa K, Tsutsumi C, Kojidani T, Sato M, Haraguchi T, Hiraoka Y. Membrane proteins Bqt3 and -4 anchor telomeres to the nuclear envelope to ensure chromosomal bouquet formation. *J Cell Biol.* 2009; 187:413–27.
<https://doi.org/10.1083/jcb.200902122>
 PMID:19948484
83. Fujita I, Nishihara Y, Tanaka M, Tsujii H, Chikashige Y, Watanabe Y, Saito M, Ishikawa F, Hiraoka Y, Kanoh J. Telomere-nuclear envelope dissociation promoted by Rap1 phosphorylation ensures faithful chromosome segregation. *Curr Biol.* 2012; 22:1932–37.
<https://doi.org/10.1016/j.cub.2012.08.019>
 PMID:22959349
84. Svobodová Kovaříková A, Bártová E, Kovařík A, Lukášová E. Spatiotemporal mislocalization of nuclear membrane-associated proteins in γ -irradiation-induced senescent cells. *Cells.* 2020; 9:999.
<https://doi.org/10.3390/cells9040999>
 PMID:32316379
85. Kotla S, Le NT, Vu HT, Ko KA, Gi YJ, Thomas TN, Giancursio C, Lusic AJ, Cooke JP, Fujiwara K, Abe JI. Endothelial senescence-associated secretory phenotype (SASP) is regulated by Makorin-1 ubiquitin E3 ligase. *Metabolism.* 2019; 100:153962.
<https://doi.org/10.1016/j.metabol.2019.153962>
 PMID:31476350
86. Kotla S, Vu HT, Ko KA, Wang Y, Imanishi M, Heo KS, Fujii Y, Thomas TN, Gi YJ, Mazhar H, Paez-Mayorga J, Shin JH, Tao Y, et al. Endothelial senescence is induced by phosphorylation and nuclear export of telomeric repeat binding factor 2-interacting protein. *JCI Insight.* 2019; 4:e124867.
<https://doi.org/10.1172/jci.insight.124867>
 PMID:31045573

87. Chi Y, Welcker M, Hizli AA, Posakony JJ, Aebersold R, Clurman BE. Identification of CDK2 substrates in human cell lysates. *Genome Biol.* 2008; 9:R149.
<https://doi.org/10.1186/gb-2008-9-10-r149>
PMID:[18847512](https://pubmed.ncbi.nlm.nih.gov/18847512/)

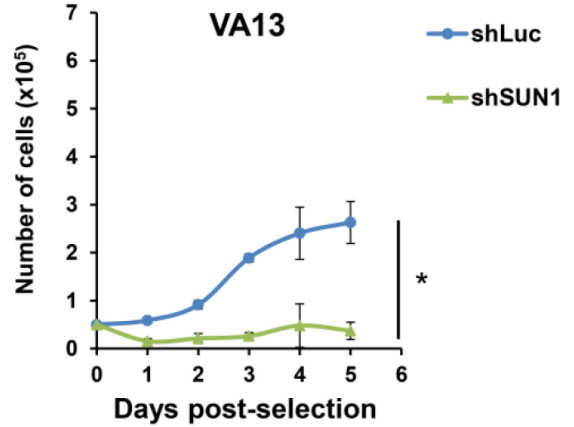
SUPPLEMENTARY MATERIALS

Supplementary Figures

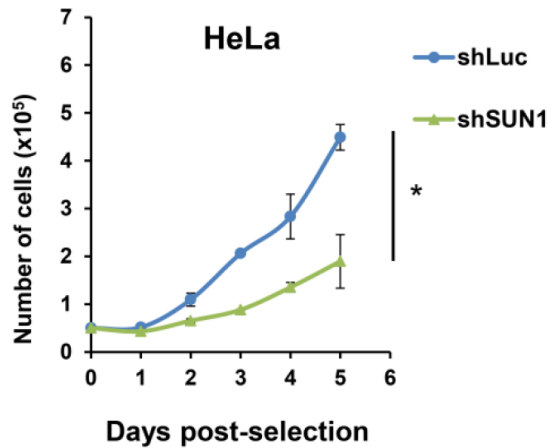
A



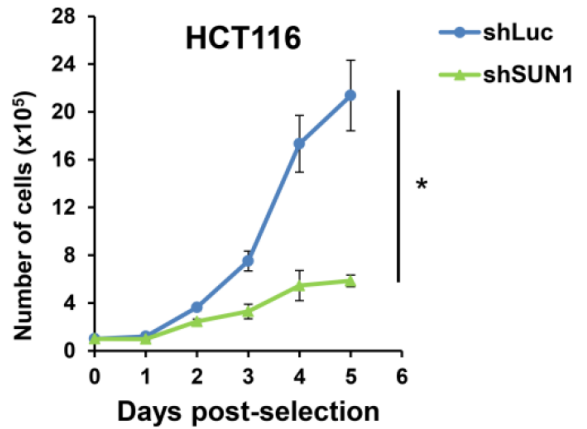
B



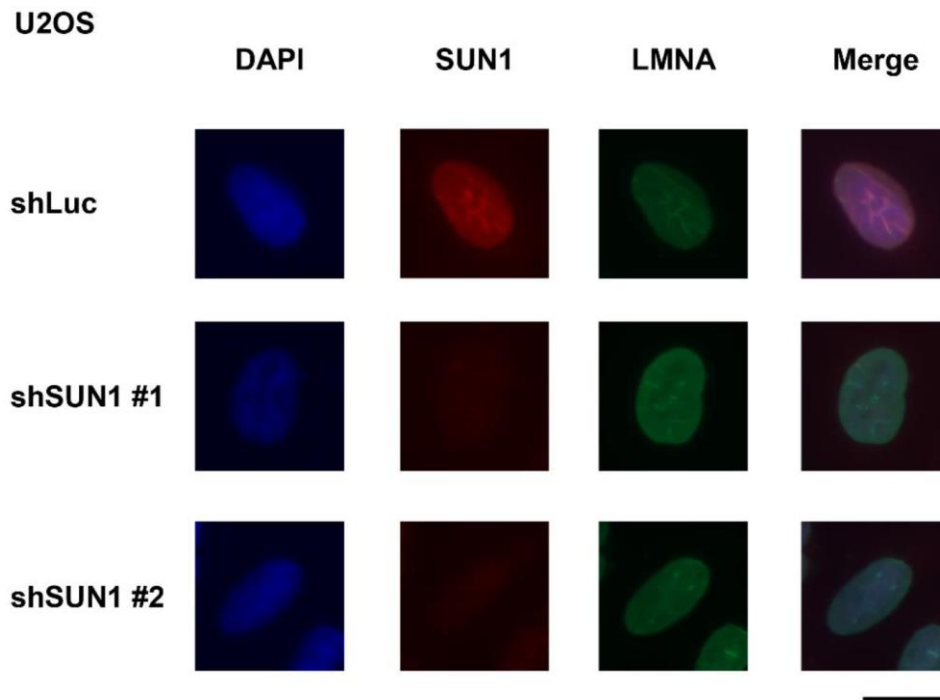
C



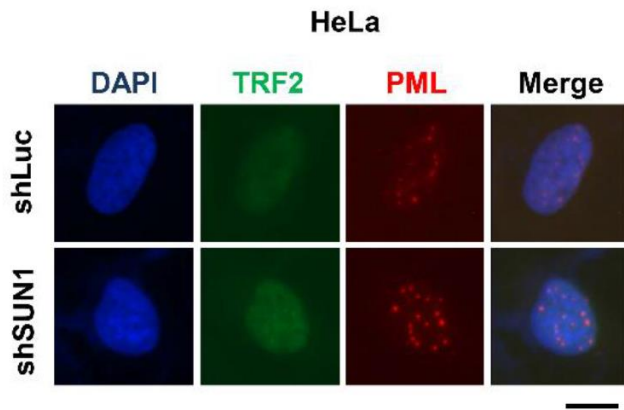
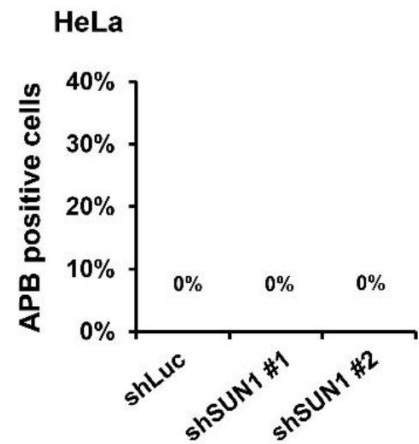
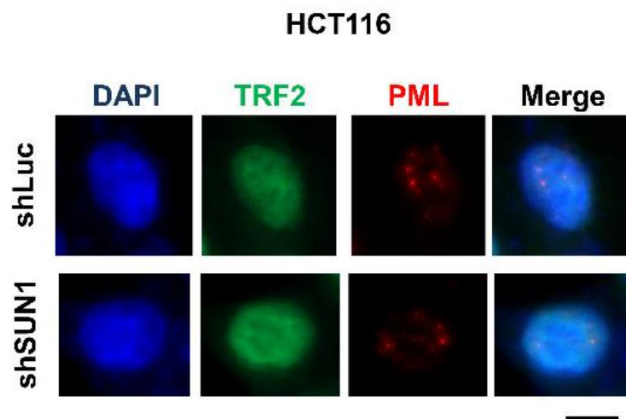
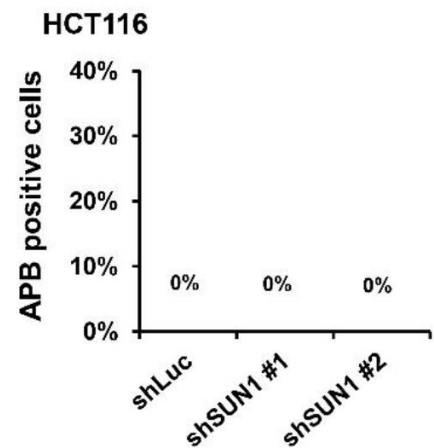
D



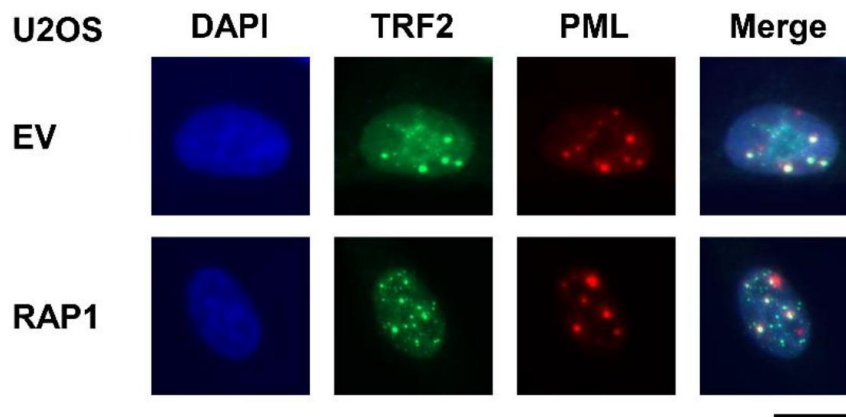
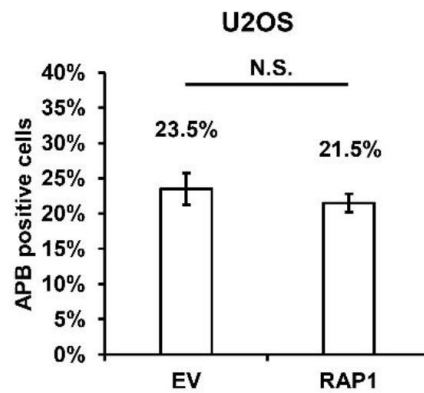
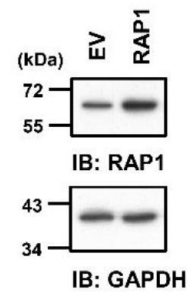
Supplementary Figure 1. Depletion of SUN1 reduces cell growth. The growth curves of the control (shLuc) and knockdown of SUN1 (shSUN1) in two telomerase-negative ALT cell lines, (A) U2OS cells and (B) VA13 cells, and two telomerase-positive cell lines, (C) HeLa cells and (D) HCT116 cells, are shown. After lentivirus infection, the cells were selected with puromycin. Cell numbers were counted during drug selection. Error bars denote SD; n=3 (independent experiments); * $P < 0.05$ (two-tailed Student's t-test).



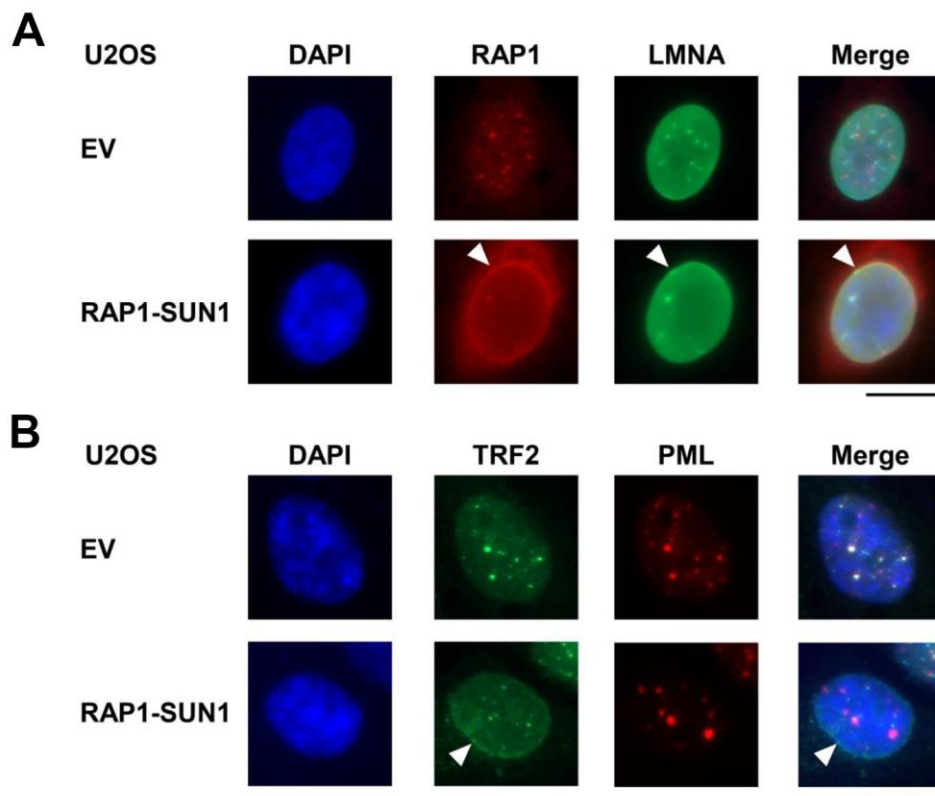
Supplementary Figure 2. Cells with SUN1 depleted maintain the intact structure of the nuclear lamina. U2OS cells were infected with control (shLuc) or shSUN1 lentiviruses and selected with puromycin for 3 days. The cells were used to perform immunofluorescence assays with anti-SUN1 (EPR6554, ab124770, Abcam) and anti-Lamin A/C (N-18, sc-6215) antibodies. DNA was stained with DAPI. Scale bar, 20 μ m.

A**B****C****D**

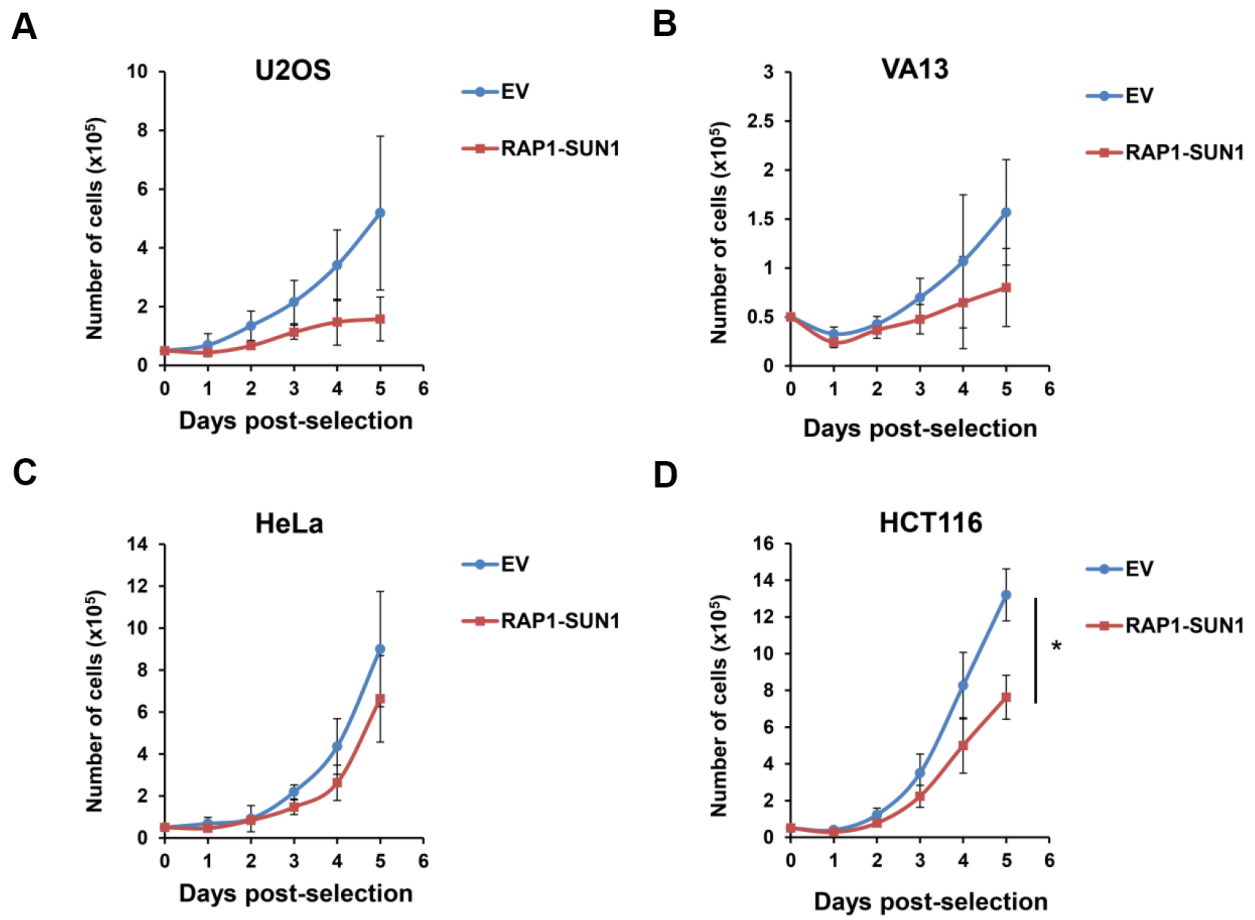
Supplementary Figure 3. Depletion of SUN1 does not induce APB formation in telomerase-positive cells. Telomerase-positive HeLa and HCT116 cells were infected with control (shLuc) or SUN1 knockdown (shSUN1) lentiviruses and selected with puromycin for 3 days. Representative images show that no APB foci were formed in the SUN1-depleted (A) HeLa cells or (C) HCT116 cells. Quantifications of APBs (%) in the (B) HeLa cells and (D) HCT116 cells were shown, respectively. Approximately 200-300 cells were analyzed for each independent experiment. Error bars denote SD; n=3 (independent experiments). Scale bar, 20 μ m.

A**B****C**

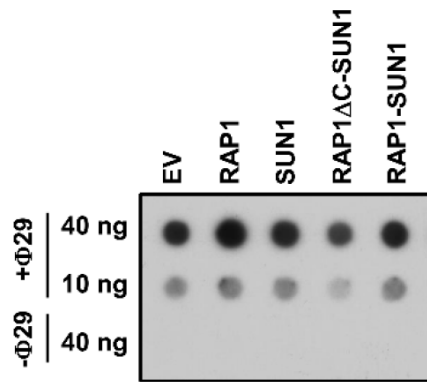
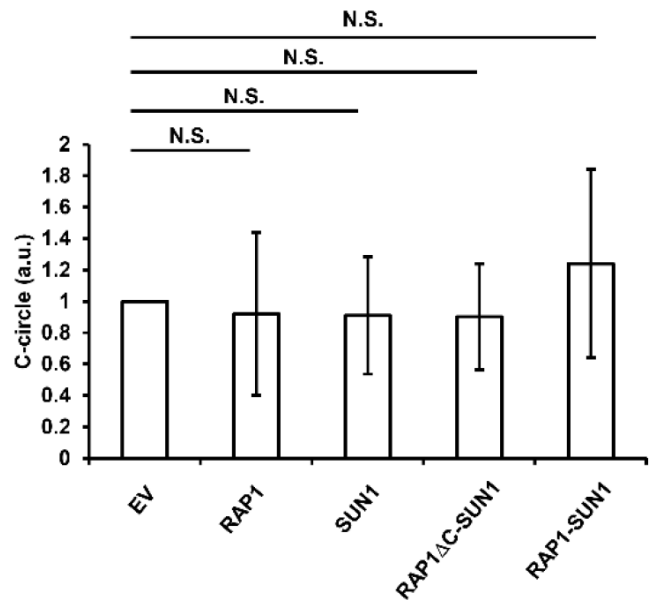
Supplementary Figure 4. Overexpression of the RAP1 protein alone does not significantly reduce the APB formation. (A) Representative images show the APBs formed in empty vector control (EV)-expressing or RAP1-expressing U2OS cells. Immunostaining was performed as described in Figure 1. Scale bar, 20 μ m. (B) Quantification of APBs (%) in the U2OS cells shown in (A). Approximately 200-300 cells were analyzed for each independent experiment. Error bars denote SD; n=3 (independent experiments); N.S., no significance (two-tailed Student's t-test). (C) Cell lysates were immunoblotted with anti-RAP1 and anti-GAPDH antibodies. GAPDH was used as the loading control.



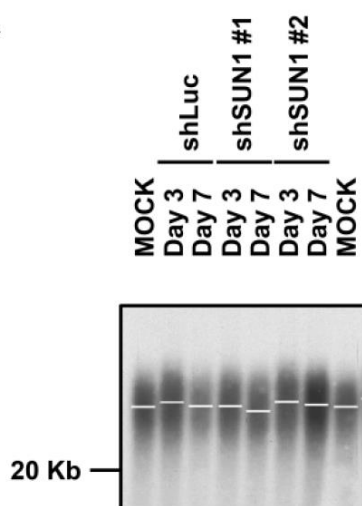
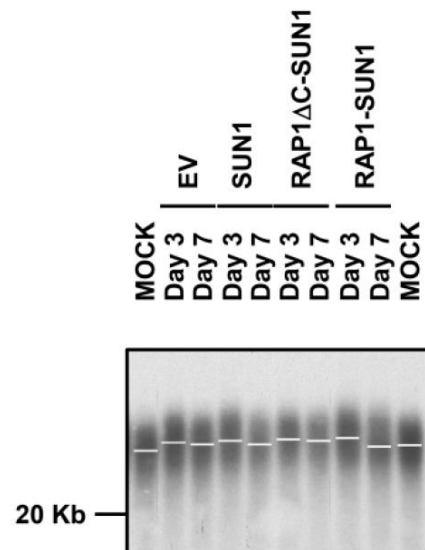
Supplementary Figure 5. RAP1-SUN1 fusion proteins are located around the periphery of the nucleus and competent to recruit TRF2. U2OS cells were infected with lentivirus expressing the empty vector control (EV) or RAP1-SUN1 fusion protein and then selected in medium containing G418- for 5 days. **(A)** Representative images show the colocalization of RAP1-SUN1 and Lamin A/C in U2OS cells. The arrowhead indicates the colocalization site. **(B)** Representative images show that TRF2 appears around the nuclear periphery in the RAP1-SUN1-overexpressing U2OS cells (arrowhead). Scale bar, 20 μ m.



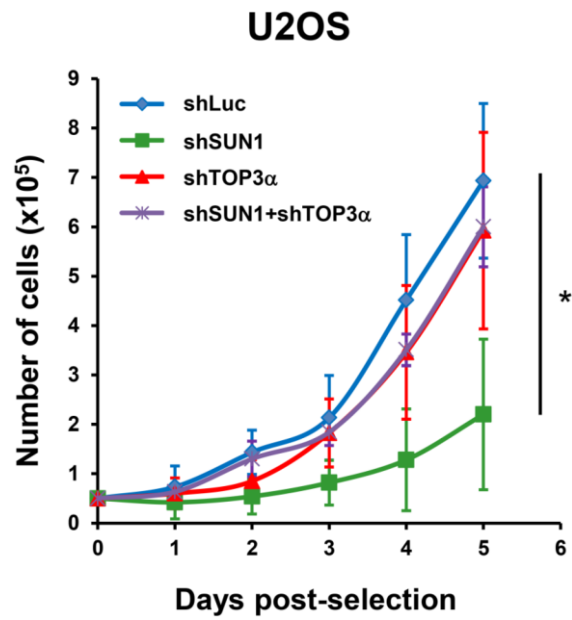
Supplementary Figure 6. Expression of the RAP1-SUN1 fusion protein reduces cell growth. The growth curves of cells expressing the empty vector (EV) or RAP1-SUN1 fusion protein (RAP1-SUN1) in two telomerase-negative ALT cell lines, (A) U2OS cells and (B) VA13 cells, and two telomerase-positive cell lines, (C) HeLa cells and (D) HCT116 cells, are shown. After lentivirus infection, cells were the selected for G418. Cell numbers were counted during drug selection. Error bars denote SD; n=3 (independent experiments); * $P < 0.05$ (two-tailed Student's t-test).

A**B**

Supplementary Figure 7. Overexpression of the RAP1-SUN1 fusion protein did not significantly change the C-circle level in U2OS cells. (A) The C-circle level in U2OS cells expressing the empty vector (EV), RAP1, SUN1, RAP1ΔC-SUN1, or RAP1-SUN1 fusion protein. (B) Quantification of the level of C-circles shown in (A). The C-circle signals were quantified with ImageJ software. The level of C-circles is represented in an arbitrary unit (a.u.). Error bars denote SD; n=3 (independent experiments); N.S., no significance (two-tailed Student's t-test).

A**B**

Supplementary Figure 8. Knockdown or overexpression of SUN1 does not disturb the homeostasis of telomere length in cells in short-term culture. (A) U2OS cells were infected with control (shLuc) or SUN1-knockdown (shSUN1) lentiviruses. The cells were selected with 1 μg/ml puromycin for 3 days and 7 days, respectively. Telomere length was measured by TRF assay. The peak intensity of telomere length is indicated by a white line. (B) U2OS cells were infected with lentiviruses overexpressing the control (EV), SUN1, RAP1ΔC-SUN1 fusion, or RAP1-SUN1 fusion protein. The cells were selected, and telomere length was measured as described in (A).



Supplementary Figure 9. Growth curves of the shLuc, shSUN1, shTOP3 α , and shSUN1+shTOP3 α ALT cells. The growth curves of U2OS cells within 5 days postselection are shown. Error bars denote SD; n=3 (independent experiments); * $P < 0.05$ (two-tailed Student's t-test).

Supplementary Tables

Supplementary Table 1. Oligo sequences for shRNA-mediated gene knockdown.

| Clone ID | Gene symbol | Target sequence | Region |
|----------------|-----------------------|-----------------------|--------|
| TRCN0000279614 | <i>SUN1</i> | GAACTAGAACAGACCAAGCAA | CDS |
| TRCN0000133655 | <i>SUN1</i> | GCTGTTCTGAACTTACGAAA | CDS |
| TRCN0000049297 | <i>TOP3A</i> | GCTTCTCGAAAGTTGAGAATA | CDS |
| TRCN0000295900 | <i>TERF2IP (RAP1)</i> | GAGAGTTCTTGCATTGGAAC | 3'UTR |

Supplementary Table 2. Primers used in this study.

| Primer | Sequence |
|--------------------|--|
| | pLAS5w-RAP1 |
| RAP1-NheI-For | CCACGTGGCGATCGCTAGCGCCACCATGGCGGAGGCGATGGATTTGGGCAAAGACCCCAA |
| RAP1-NsiI-Rev | CTGTACATGCATTTATTTCTTTCTAAATTCAATCCTCCGAGCTACATTCTGAGCACC |
| | pLAS5w-SUN1 |
| NheI-SUN1-For | GCTAGCATGGATTTTTCTCGGCTTCA |
| SUN1-EcoRI-Rev | GAATTCTCACTTGACAGGTTCCGCAT |
| | pLAS5w-RAP1-SUN1 |
| HpaI-RAP1-For | GTTAACATGGCGGAGGCGATGGATTT |
| RAP1-G8-NheI-Rev | GCTAGCACCACCACCACCACCACCACCTTTCTTTTCGAAATTCAATCC |
| NheI-SUN1-For | GCTAGCATGGATTTTTCTCGGCTTCA |
| SUN1-EcoRI-Rev | GAATTCTCACTTGACAGGTTCCGCAT |
| | pLAS5w-RAP1 ΔC-SUN1 |
| HpaI-RAP1-For | GTTAACATGGCGGAGGCGATGGATTT |
| RCTdel-G8-NheI-Rev | GCTAGCACCACCACCACCACCACCACCACC TGAGTCTTCCTCAGGTGTGGGTGGATCATC |
| | pcDNA3HA-RAP1 |
| RAP1-BamHI-1F | GGATCCAATGGCGGAGGCGATGGATTTG |
| RAP1-XhoI-R | CTCGAGTTATTTCTTTTCGAAATTC |
| | pcDNA3HA-RAP1 ΔN |
| hRAP1-BamHI-129F | GGATCCACGGCAGCCGGGCGGATC |
| RAP1-XhoI-R | CTCGAGTTATTTCTTTTCGAAATTC |
| | pcDNA3HA-RAP1 ΔMyb |
| Mybdel-F | AGCCGCAGCGGCACGCCGGGAGCATAAGTACCTGCTGGGGGACG |
| Mybdel-R | CCCAGCAGGTAATTATGCTCCCCGGCGTGCCGCTGCGGCTCCGGC |
| | pcDNA3HA-RAP1 ΔCoil and pLAS5w-RAP1 ΔCoil |
| Coildel-F1 | GACCGCTACCTCAAGCACCTGCGGGGCCAGGACTCAGAAACACAGCCTGATGAGGAGGAA |
| Coildel-R1 | TTCTCCTCATCAGGCTGTGTTTCTGAGTCTGGCCCCGAGGTGCTTGAGGTAGCGGTC |
| | pcDNA3HA-RAP1 ΔC |
| RAP1-BamHI-1F | GGATCCAATGGCGGAGGCGATGGATTTG |
| hRAP1-XhoI-289R | CTCGAGTTATTCCTCAGGTGTGGGTGG |